Epitaxial growth of magnetic-oxide thin films

6

J.A. Moyer[1], *R.V.K. Mangalam*[1], *L.W. Martin*[2,3]
[1]University of Illinois, Urbana-Champaign, IL, USA; [2]University of California, Berkeley, CA, USA; [3]Lawrence Berkeley National Laboratory, Berkeley, CA, USA

6.1 Introduction

Complex oxides represent a vast class of materials encompassing a wide range of crystal structures and functionalities. Amongst these interesting properties, the study of ferroic order (namely ferromagnetic, ferroelectric, ferroelastic, and multiferroic properties) has driven considerable research over the past few decades. Driven by the development of new synthesis techniques—especially for thin films—the field of functional oxide materials has experienced unprecedented growth in terms of the discovery of new materials systems, characterization and understanding of the fundamental properties and nature of existing systems, and in the control of properties in these materials through elegant changes in crystal chemistry (i.e., doping), strain, and other variables. Throughout this book, many examples of how these aspects can be applied to complex-oxide materials have been developed. In this chapter, in turn, we focus on advances in the growth and characterization of magnetic oxide materials while investigating the structure, properties, and synthesis of modern magnetic complex-oxide thin films. We will investigate a number of prototypical examples of materials within this subgroup of ferroic oxides and will delve into the coupling of epitaxial constraint and magnetic properties and how this diverges from bulk materials.

6.2 Magnetism and major magnetic-oxide systems

6.2.1 Magnetism in oxides

Magnetic materials violate time-reversal symmetry, but are invariant under spatial inversion; in other words, when magnetic moments are present in a crystal, the antisymmetry operator must also be present. The 32 classical crystallographic point groups do not have the antisymmetry operator and hence cannot fully describe the symmetry of magnetic crystals. Symmetry analysis reveals 122 total magnetic space groups of which only 31 can support ferromagnetism (Aizu, 1970; Laughlin, Willard, & McHenry, 2000). A material is said to be a ferromagnet when there is long-range, parallel alignment of the atomic moments resulting in a spontaneous net magnetization even in the absence of an external field. Ferromagnetic materials undergo a phase transition from a high-temperature phase that does not have macroscopic magnetization

Epitaxial Growth of Complex Metal Oxides. http://dx.doi.org/10.1016/B978-1-78242-245-7.00006-3

(atomic moments are randomly aligned resulting in a *paramagnetic* phase) to a low-temperature phase that does at the so-called Curie temperature (T_C). There are other types of magnetism including antiferromagnetism (atomic moments are aligned anti-parallel) and ferrimagnetism (dipoles align anti-parallel, but one subset of dipoles is larger than the other, resulting in a net moment). The theory of magnetism is a rich field and beyond the scope of this chapter, but is built upon the idea of quantum mechanical exchange energy, which causes electrons with parallel spins and therefore parallel moments to have lower energy than spins with anti-parallel spin. Magnetic materials find pervasive use in all walks of life, from information technology (storage, sensing. and communications) to health sciences (e.g., cancer treatment) and beyond.

A history of magnetism is a history of oxide materials. From casual observations in antiquity (it is said that the Greek philosopher Thales of Miletus, 634−546 BC, is thought to be the first person to describe magnetism after observing the attraction of iron by the mineral magnetite) to an enabling force for developing the world (including navigation, power production, and more), magnetic oxides have played a key role over the years. For a complete history of magnetism in materials see Verschuur (1993). Of particular interest for the first few thousand years of the study of magnetism, there was only one material, which came to be known as lodestone (in old English, "lode" is the word for lead) or the iron-oxide phase magnetite (Fe_3O_4). Only after 1819 did a rapid expansion of our knowledge of magnetic materials occur. Only after the development of a spin-dependent model for the exchange interaction in 1928 by Heisenberg was it possible, however, to understand the nature of magnetic oxides that had dominated the landscape for the previous millennia. From that point on, the understanding of magnetism in oxides developed at a feverish pace. Of fundamental importance to this early work was a series of publications by Lois Néel, who developed the idea of antiferromagnetism (Néel, 1932). By the late 1950s, a rapid expansion of technology, especially high-frequency devices, stimulated rapid research in ferromagnetic oxides, and Smit and Wijn in their book on ferrites noted that in 1959 the properties of magnetic oxides were better understood than the properties of metallic ferromagnets (Smit & Wijn, 1959).

What arose from this work was an understanding that magnetism in oxides is fundamentally different from that in metallic, elemental systems. Magnetism in oxides is generally mediated through indirect exchange (through nonmagnetic anions), which gives rise to interesting coupling effects, including, for example, superexchange, double exchange, and RKKY coupling (named after the work of Ruderman and Kittel (1954), Kasuya (1956), and Yosida (1957)). Briefly, superexchange gets its name from the fact that it extends the normally very-short-range exchange interaction to a longer range (Stöhr & Siegmann, 2006). The idea that exchange could be mediated by an intermediate, nonmagnetic atom was put forth in 1934 (Kramers, 1934), and the theory was formally developed by Anderson in 1950 (Anderson, 1950). Superexchange is an important effect in ionic solids where $3d$ and $2p$ orbitals of transition metal cations (*TM*) and anions interact, and it describes, through a simple valence-bonding argument, how antiferromagnetic (AF) ordering occurs. Double exchange, first proposed by Zener in 1951 (Zener, 1951), describes the magneto-conductive properties of these mixed-valence compounds and delineates the mechanism for hopping

of an electron from one site to another through the mediating oxygen atom. Because the O^{2-} ion has full *p*-orbitals, the movement from one ion through O^{2-} to another ion is done in two steps. The electron is thus delocalized over the entire *TM*−O−*TM* group, and the cations are said to be of mixed valence. This is aided by the fact that spin-flips are not allowed in electron-hopping processes, and thus it is more energetically favorable if the magnetic structure of the two cations is identical; therefore, ferromagnetic alignment of moments is achieved. Finally, RKKY exchange is not based on the relationship between bonding and magnetism, but instead is the concept that a local moment can induce a spin polarization in a surrounding conduction electron sea. Studies showed that the spin polarization of the conduction electrons oscillates in sign as a function of distance from the localized moment, and this spin information can be carried over relatively long distances.

6.2.2 Early work on epitaxy of magnetic oxides

Considerable work has been done on magnetic oxide films. Again, complex oxides exhibit a wide range of physical phenomena due to the interaction of the lattice with the charge, spin, and orbital degrees of freedom (Dagotto, 2005; Lu, West, & Wolf, 2010; Tokura & Nagaosa, 2000). More practically, magnetic oxides have been investigated for their potential in applications such as magnetoresistive random access memories and spin valves (Coey, Venkatesan, & Xu, 2013; Mallinson, 1993; Zubko, Gariglio, Gabay, Ghosez, & Triscone, 2011). They possess a wide range of crystal structures and chemistries (including binary oxides such as MO, MO_2, and M_2O_3) (Martin, Chu, & Ramesh, 2010). Popular monoxide systems include the dilute magnetic oxide semiconductors (i.e., transition-metal cation-doped ZnO) (Özgür et al., 2005). Binary dioxides such as CrO_2 have large spin polarizations and are promising materials for use in spintronics (Lu et al., 2010; Coey et al., 2013). Binary trivalent oxides such as Fe_2O_3 have been investigated for integration in magnetic media (Mallinson, 1993). Recent advances in thin-film growth have greatly expanded the number of materials for magnetic devices to include perovskite manganites and spinel ferrites (Lu et al., 2010; Wolf et al., 2001) and single-phase and composite/two-phase multiferroics for magnetoelectrics (Catalan & Scott, 2009; Chu et al., 2008; Chu, Martin, Holcomb, & Ramesh, 2007; Eerenstein, Mathur, & Scott, 2006; Prellier, Singh, & Murugavel, 2005; Ramesh & Spaldin, 2007; Seidel et al., 2012; Yu, Chu, & Ramesh, 2012).

6.2.3 Recent advances in thin film epitaxy

Although there is a considerable amount of excellent work on epitaxial magnetic-oxide thin films, here we focus on a few select systems to highlight the major players and developments and understanding of magnetism in thin films.

6.2.3.1 Perovskite manganites

The perovskite manganites are represented by the general formula $RE_{1-x}A_xMnO_3$ (RE = rare earth metal cation, A = alkaline earth metal cation). Due to strong electron

correlations that couple the charge, spin, and lattice (Tokura & Nagaosa, 2000), they can display magnetic, colossal magnetoresistant, half-metallic, and charge-ordering behaviors (Dagotto, 2003; Jonker & Van Santen, 1950; Rao & Raveau, 1998; Tokura, 2000). $La_{1-x}Sr_xMnO_3$ with $x = 0.3$ is the most widely studied perovskite manganite due to its room-temperature ferromagnetism and metal−insulator transition (Urushibara et al., 1995). A large availability of perovskite substrates has enabled the understanding of the physics behind the complex phenomena of the manganites (Martin et al., 2010), where epitaxial strain has been utilized to tune their properties (Haghiri-Gosnet & Renard, 2003; Prellier, Lecoeur, & Mercey, 2001). For example, the magnetic easy axis of $La_{0.7}Sr_{0.3}MnO_3$ film can be tuned to be along the in-plane or out-of-plane direction by applying tensile or compressive strain, respectively (Kwon et al., 1997). In recent years, thickness-dependent studies on $La_{0.7}Sr_{0.3}MnO_3$ films identified the presence of a three-unit cell ($\sim$12 Å) dead layer, which is a layer that exhibits neither metallicity nor ferromagnetism (Figure 6.1) (Huijben et al., 2008).

6.2.3.2 Perovskite nickelates

Research on perovskite nickelates has gone through a recent resurgence due to its metal−insulator and AF−paramagnetic phase transitions (Catalan, 2008; María Luisa, 1997). Nickelates are interesting candidates for many technological applications (Aydogdu, Ha, Viswanath, & Ramanathan, 2011; Lee et al., 2007; Meijer, 2008; Takagi & Hwang, 2010; Yang, Ko, & Ramanathan, 2011) such as sensors, electronic switches, and thermochromic coatings. The ideal structure consists of NiO_6^{3-} octahedra linked at their corners with R^{3+} cations. The R^{3+} cations are accommodated through rigid rotations of the NiO_6^{3-} octahedra, resulting in a decrease of the Ni−O−Ni bond angle away from 180°. The electronic and magnetic phase transitions arise from the sensitivity of the interaction between the Ni-3*d* and O-2*p* electrons and the bond angle (Disa et al., 2013; María Luisa, 1997). By selecting a suitable R^{3+} cation or solid solution of rare earths, the metal−insulator transition temperature (T_{MI}) can be continuously tuned from 0 K for $LaNiO_3$ to 600 K for $LuNiO_3$ (Alonso, Martínez-Lope, Casais, Aranda, & Fernández-Díaz, 1999; Torrance, Lacorre, Nazzal, Ansaldo, & Niedermayer, 1992). In addition to temperature, epitaxial strain can also be used to control the phase transitions. For $NdNiO_3$ films, for instance, T_{MI} increases (decreases) under tensile (compressive) strain, an effect that is attributed to an increase (decrease) of the Ni−O−Ni bond angle (Conchon et al., 2007; Disa et al., 2013; Eguchi et al., 2009; Kumar, Choudhary, & Kumar, 2012; Liu et al., 2010; Novojilov et al., 2000; Tiwari, Jin, & Narayan, 2002). It has alternatively been suggested that tensile in-plane stress may lead to a novel breathing distortion that creates two unequivalent Ni sites and an increase in T_{MI} (Chakhalian et al., 2011).

6.2.3.3 Perovskite cobaltites and ruthenates

In addition to being promising candidates for ionic conductors and surface catalysts for the fuel-cell industry (Choi et al., 2012; Han & Yildiz, 2011; Mehta et al., 2009;

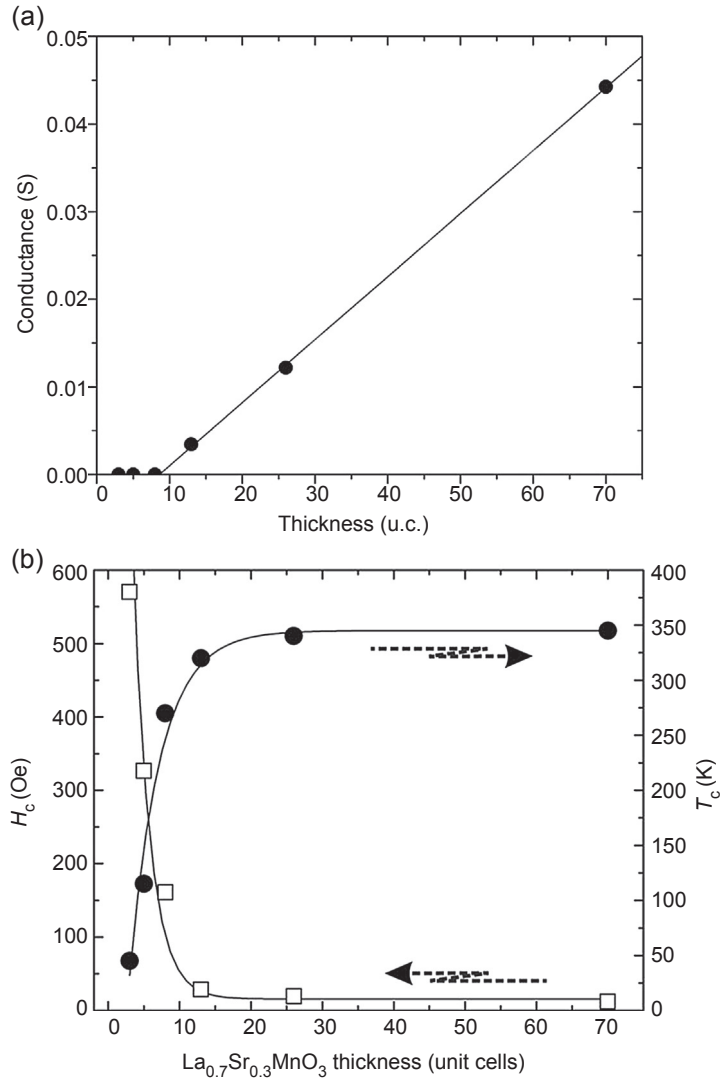

Figure 6.1 Thickness dependence of the (a) total conductance of $La_{0.7}Sr_{0.3}MnO_3$ films at 10 K and (b) the coercive fields (H_C) and Curie temperatures (T_C).
Adapted from Huijben et al. (2008).

Sharma, Gazquez, Varela, Schmitt, & Leighton, 2011), the cobaltites also have interesting physics associated with their magnetic spins (Sterbinsky et al., 2012). $LaCoO_3$ has been studied intensely over the last 50 years due to two broad transitions in its magnetic susceptibility ($T_C \sim 80$ K) and its subsequent nonmetal−metal transition ($T \sim 500$−600 K); the origin of the two magnetic transitions in $LaCoO_3$ is controversial (Klie, Yuan, Tanase, Yang, & Ramasse, 2010). In addition, the ferroelastic

properties of $LaCoO_3$ (Choi et al., 2012; Kleveland et al., 2001; Vullum et al., 2007; Vullum, Lein, Einarsrud, Grande, & Holmestad, 2008) make it intriguing for studying the strain coupling of the structural, electronic, ionic, and magnetic properties, where the strain can be used as a tool to control the ionic activities as predicted by density functional theory (Han & Yildiz, 2011; Kushima, Yip, & Yildiz, 2010). The ruthenates, such as $SrRuO_3$, are another magnetic oxide system that has a perovskite structure (Choi, Eom, Rijnders, Rogalla, & Blank, 2001; Eom, 1997; Hong et al., 2005), and are well studied for their use in magnetic tunnel junctions (MTJs) and as electrodes (Koster et al., 2012).

6.2.3.4 Double perovskites

The double perovskite is a variant of the perovskite structure having a unit cell doubled in all three directions. This gives rise to two different octahedrally coordinated cations, which form a NaCl-type superlattice (Coey, Viret, & von Molnár, 1999). A large spin polarization, close to 100%, in double perovskites like Sr_2FeMoO_6 (Kobayashi, Kimura, Sawada, Terakura, & Tokura, 1998) and Sr_2FeReO_6 (Kobayashi et al., 1999), makes them interesting for spintronic applications (Philipp et al., 2001). Recently, metastable Bi_2NiMnO_6 was synthesized under high pressure and temperature and measured to be multiferroic, with a ferromagnetic transition temperature of 140 K and a ferroelectric transition temperature of 485 K (Azuma et al., 2005). In contrast to the weak ferromagnetism in typical oxide multiferroics, like $BiFeO_3$, Bi_2NiMnO_6 has a large moment due to ferromagnetically coupled Ni^{2+} and Mn^{4+} spins. A thin film of metastable Bi_2NiMnO_6 was epitaxially grown on $SrTiO_3$ substrates with pulsed laser deposition and was reported to have the rock salt-type arrangement of Ni^{2+} and Mn^{4+} cations indicative of a double perovskite unit cell (Sakai et al., 2007).

6.2.3.5 Hexagonal oxides

Sufficiently small cationic radii compounds with the general formula ABO_3 or $A_2BB'O_6$ may crystallize in a hexagonal rather than the typical perovskite structure (Manfred, 2005). Researchers have focused on the hexagonal multiferroics (Cheong & Mostovoy, 2007; Das, Wysocki, Geng, Wu, & Fennie, 2014; Fiebig, Lottermoser, Frohlich, Goltsev, & Pisarev, 2002; Kimura et al., 2003; Lee et al., 2008; Lueken, 2008; Van Aken, Palstra, Filippetti, & Spaldin, 2004), that is, the ferroelectric−AF manganites ($RMnO_3$ with R = Sc, Y, In, Ho, Er, Tm, Yb, Lu), which can possess four long-range ordered subsystems: a ferroelectric lattice with $T_C \approx 570-990$ K, an AF Mn^{3+} lattice with Néel temperatures of 70−130 K, and two rare-earth sublattices with magnetic ordering temperatures of ~5 K. In contrast to the perovskites, relatively few examples of element substitution have been reported (Manfred, 2005). Utilizing advances in film growth, researchers reported the observation of nanoscale strain gradients (10^5-10^6 per meter) in ferroelectric $HoMnO_3$ films, resulting in giant flexoelectric effects (Lee et al., 2011).

6.2.3.6 Oxide spinels, garnets, and other crystal structures

The spinel ferrites, $TMFe_2O_4$ (TM = transition-metal cation), are multivalent oxides that crystallize in the spinel structure, in which one-third of the cations occupy tetrahedral sites (A sites) and two-thirds of the cations occupy octahedral sites (B sites). If the divalent cations occupy A sites (B sites), the crystal structure is called normal (inverse) spinel. The parent compound Fe_3O_4 is fully inverse, $CoFe_2O_4$ and $NiFe_2O_4$ are predominantly inverse, and $MnFe_2O_4$ and $ZnFe_2O_4$ are predominantly normal. The majority of the spinel ferrites are ferrimagnets ($ZnFe_2O_4$ is AF), in which the A and B sites are aligned antiferromagnetically with each other (Figure 6.2), and can possess a T_C much higher than room temperature (e.g., 858 K for Fe_3O_4) (Slick, 1980). MgO is the only substrate that is well lattice-matched with the spinel ferrites; however, it presents two drawbacks. First, Mg^{2+} cations easily diffuse into the films at temperatures above 350 °C, which necessitates low growth temperatures (Gao, Kim, & Chambers, 1998). Second, the cubic lattice parameter for MgO is approximately one-half of that of the ferrites, resulting in the formation of anti-phase boundaries in the films and domains that can be structurally out-of-phase (Margulies et al., 1997). Spinel ferrites can be grown on other substrates, although they quickly relax, contain many defects, and typically have rough surfaces. Films grown on perovskite substrates have large lattice mismatches (~7%) and contain anti-phase boundaries; whereas films grown on $MgAl_2O_4$ also have large lattice mismatches (~5%) but do not have anti-phase

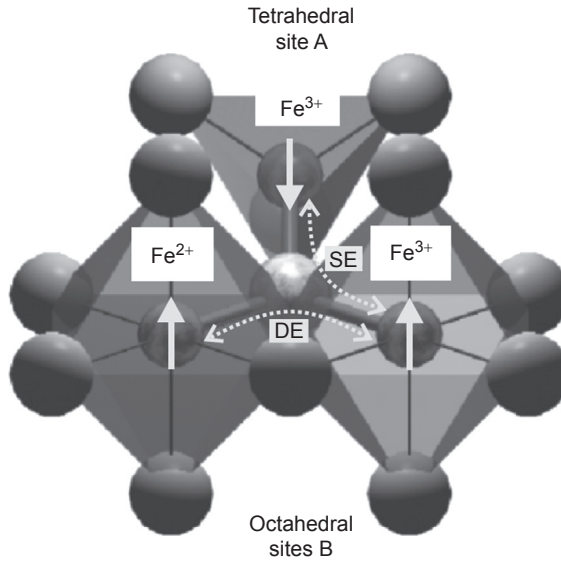

Figure 6.2 Model of magnetic interactions in Fe_3O_4, demonstrating how both superexchange (SE) and double exchange (DE) interactions give rise to a ferrimagnetic magnetic ordering between the tetrahedral (A site) and octahedral (B site) sublattices.
From Stöhr and Siegmann, (2006).

boundaries. Crystallinity and magnetic properties of thin films grown on $MgAl_2O_4$ and $SrTiO_3$ can be improved using buffer layers such as $CoCr_2O_4$ in order to alleviate the majority of the strain (Suzuki et al., 1996). Many other magnetic oxide crystals structures exist, although, they are not commonly grown as epitaxial thin films; some that can be grown epitaxially are the spinel chromates (i.e., $CoCr_2O_4$) and garnets (i.e., $Y_3Fe_5O_{12}$).

6.2.3.7 Multiferroics

Multiferroics (Schmid, 1994) are materials that simultaneously possess two or more of the so-called ferroic-order parameters: ferroelectricity, ferromagnetism, and ferroelasticity. They have grown in interest because of the potential for strong coupling between ferroelectric and ferromagnetic-order parameters, enabling simple control over the magnetic nature of the material with an electric field. For instance, $BiFeO_3$ is one of the few single-phase multiferroics that simultaneously possesses both magnetic and ferroelectric order at and above room temperature. $BiFeO_3$ is a G-type AF (Kiselev, Ozerov, & Zhdanov, 1963; Teague, Gerson, & James, 1970) with a Néel temperature of $\sim$673 K (Fischer, Polomska, Sosnowska, & Szymanski, 1980) that, in the bulk, possesses a cycloidal spin structure with a period of $\sim$620 Å (Sosnowska, Peterlinneumaier, & Steichele, 1982). Additionally, the magnetic moments are oriented perpendicular to the <111>-polarization direction, and the symmetry also permits a small canting of the moments in the structure, resulting in a weak canted ferromagnetic moment of the Dzyaloshinskii–Moriya type (Dzyaloshinskii, 1957; Moriya, 1960). Extensive work on thin films of $BiFeO_3$ has been completed and dramatic changes in the magnetic order are possible with thin-film strain (Holcomb et al., 2010; Martin et al., 2010; Martin & Ramesh, 2012; Martin & Schlom, 2012; Sando et al., 2013). Other multiferroics studied as thin films includes the rare-earth manganites ($REMnO_3$), which depending on the size of the *RE* ion, take on either orthorhombic (*RE* = Dy, Tb, and Gd) (Kimura et al., 2003; Kimura, Lawes, Goto, Tokura, & Ramirez, 2005) or hexagonal (*RE* = Ho–Lu, as well as Y) (Lottermoser et al., 2004) structures (Yakel, Forrat, Bertaut, & Koehler, 1963). The $REMn_2O_5$ (*RE* = rare earth, Y, and Bi) family of materials (Shukla et al., 2009) has also been investigated in ultrathin layers (Sai, Fennie, & Demkov, 2009), been used to demonstrate electric field control of exchange-coupled ferromagnets (Skumryev et al., 2011), and been investigated for effects of non-stoichiometry and solubility limits (Gélard et al., 2011). $BiMnO_3$ has received considerable attention since it is not a stable phase at 1 atm pressure and thus epitaxial stabilization can be used to create metastable films of this material (Ohshima, Saya, Nantoh, & Kawai, 2000). $BiMnO_3$ film has been used as the foundation for a four-state memory concept (Gajek et al., 2007) and has been shown to exhibit large magnetodielectric effects (Yang, Lee, Koo, & Jeong, 2007). There are a number of other candidate multiferroic materials that have been studied as thin films, including $BiCrO_3$ (Hill, Battig, & Daul, 2002; Kim, Lee, Varela, & Christen, 2006; Murakami et al., 2006), $PbVO_3$ (Kumar et al., 2007; Martin et al., 2007), and Bi_2NiMnO_6 (Sakai et al., 2007) as examples.

6.3 The effects of thin-film epitaxy on magnetism

The greater field of magnetism is rich with thin-film phenomena (Bader, 1990). From magnetic size effects including diminished magnetization in ultrathin films, decreased magnetocrystalline anisotropy, and epitaxial strain-induced changes in properties, one must consider the effects of changing material geometry and the elastic boundary conditions on the evolution of magnetic properties.

6.3.1 Size effects

6.3.1.1 Magnetic dead layers in $La_{0.7}Sr_{0.3}MnO_3$

Dimensionally confining the thickness of a thin film is a common approach to tune its properties, but in some magnetic oxides one must be aware of so-called magnetic dead layers. Combined spin-resolved photoemission spectroscopy, SQUID magnetometry, and X-ray magnetic circular dichroism studies have shown that there is diminished magnetism at the surface boundary of $La_{0.7}Sr_{0.3}MnO_3$ films (Park et al., 1998). Further studies found that the critical thickness for a nonmetallic and nonferromagnetic $La_{0.7}Sr_{0.3}MnO_3$ layer at the interface with $SrTiO_3$ (001) is three unit cells ($\sim$12 Å) (Figure 6.1) (Huijben et al., 2008). Spectroscopic and scattering studies on $La_{0.7}Sr_{0.3}MnO_3/SrTiO_3$ (001) revealed that the average Mn valence varies from mixed Mn^{3+}/Mn^{4+} to an enriched Mn^{3+} region near the $SrTiO_3$ interface, resulting in a compressive lattice distortion along the in-plane axes and a possible electronic reconstruction in the Mn e_g orbital ($d_{3z}^2-_r^2$) (Lee et al., 2010). This reconstruction may provide a mechanism for coupling the Mn^{3+} moments antiferromagnetically along the surface normal direction, and in turn may lead to an observed reversed magnetic configuration.

The thickness dependence of magnetism and electrical conductivity in ultrathin $La_{0.67}Sr_{0.33}MnO_3$ films grown on $SrTiO_3$ (110) substrates differs from those films grown on $SrTiO_3$ (001). In films grown on $SrTiO_3$ (110), there is a critical thickness of 10 unit cells below which the conductivity of the films disappears and simultaneously T_C increases, indicating a ferromagnetically insulating phase at room temperature (Boschker et al., 2012). These samples have a Curie temperature of about 560 K with a saturation magnetization of 1.2 ± 0.2 μ_B/Mn. The canted AF insulating phase in these films coincides with the occurrence of a higher-symmetry structural phase with a different oxygen octahedra rotation pattern. Such a strain-engineered phase is an interesting candidate for an insulating tunneling barrier in room-temperature spin filters.

6.3.1.2 Ultrathin spinel ferrite films

Spinel ferrite thin films grown on MgO and $SrTiO_3$ substrates have magnetic moments that are significantly reduced from their bulk values and do not saturate in magnetic fields up to 7 T. This was first observed in Fe_3O_4/MgO (001) heterostructures and was attributed to the presence of anti-phase boundaries (Figure 6.3) (Margulies et al., 1996, 1997) that give rise to magnetic superexchange interactions

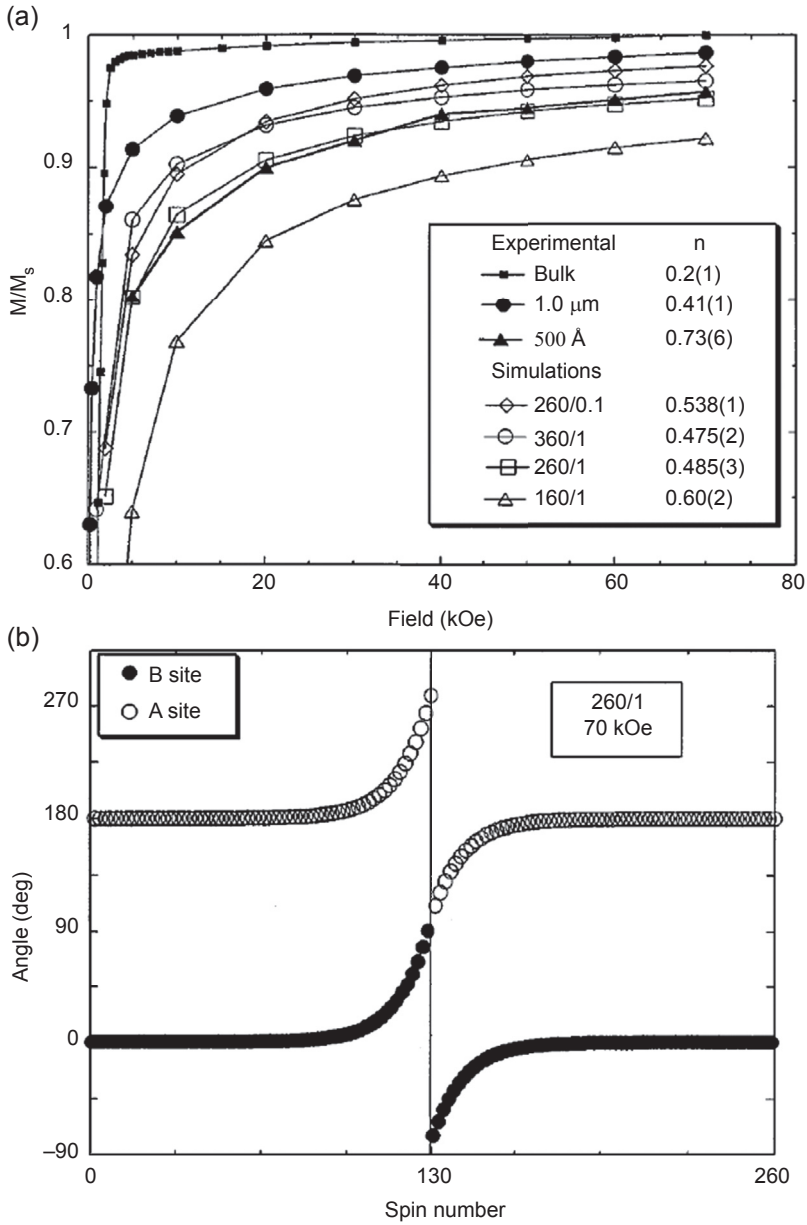

Figure 6.3 (a) Magnetization−magnetic field hysteresis loops comparing a single crystal of Fe_3O_4 with 1-μm and 50-nm thin films of Fe_3O_4 grown on MgO (001). The magnetization of the films is normalized to the bulk value and the measurement is made along the [100] crystal axis. Overlaid are simulations for a ferrimagnetic linear chain of spins with the sign of the exchange reversed at the center to simulate an anti-phase boundary. The number of spins in the chain and strength of the exchange at the center are provided. (b) The angle of spins in a linear chain of spins is given at 70 kOe.
From Margulies et al. (1997).

that do not exist in the spinel structure (Margulies et al., 1997; Celotto, Eerenstein, & Hibma, 2003). These new superexchange interactions are AF and stronger than the magnetic exchange interactions that are native to the spinel ferrites (Celotto et al., 2003), resulting in changes in the spin alignments near the anti-phase boundaries and a reduced moment. The density of anti-phase boundaries decreases as the film thickness is increased (Eerenstein, Palstra, Saxena, & Hibma, 2002; Moussy et al., 2004) and near-bulk magnetic properties are obtained for thick films (Margulies et al., 1997). The reduction in magnetic moment for other spinels can be more severe, such as in $CoFe_2O_4$, where the moment is reduced by up to 75% (Chambers et al., 2002; Moyer, Vaz, Arena et al., 2011) due to additional effects, such as its having a partially inverse spinel crystal structure (Moyer, Vaz, Arena et al., 2011).

Additionally, anomalous increases in the magnetic moments of Fe_3O_4, $CoFe_2O_4$, and $NiFe_2O_4$ films in the ultrathin limit (less than 10 nm) have been observed. The increase in the moment seems to depend on the growth technique and substrate. Films that are grown with sputtering or PLD on $SrTiO_3$ (001) substrates can have magnetic moments well above the bulk moment. For instance, 3-nm $NiFe_2O_4$ films have shown magnetic moments four times the bulk value (Luders et al., 2005). This increase in moment is attributed to cation disorder produced by the high energetics of the growth technique, resulting in the crystal structure becoming more normal spinel as the film thickness is reduced. Smaller enhancements were seen for $CoFe_2O_4$ films, with an increase in the magnetic moment of about 20% for 3.5-nm films (Rigato, Geshev, Skumryev, & Fontcuberta, 2009). Films grown by MBE on MgO (001) substrates, on the other hand, do not show increased moments in the same thickness regime. For Fe_3O_4 and $CoFe_2O_4$ films, there is evidence of superparamagnetic behavior (Moyer, Vaz, Kumah, Arena, & Henrich, 2012; Voogt et al., 1998). These films have large densities of anti-phase boundaries and a high density of domains, leading to each domain acting as an individual paramagnet (Eerenstein, Palstra, Hibma, & Celotto, 2002; Eerenstein, Hibma, & Celotto, 2004). Unlike films grown with higher-energy growth techniques on $SrTiO_3$, as described above, there is no change in the cation distribution for these films as the film thickness decreases (Moyer et al., 2012).

6.3.1.3 *Spin polarization of Fe_3O_4 and appearance of magnetic dead layer*

While magnetic measurements show no evidence of dead layers in ultrathin spinel ferrite films, spin polarization measurements of Fe_3O_4 do observe a dead layer at the surface with a thickness of 5−8 Å (Tobin et al., 2007). This dead layer arises from a surface reconstruction that occurs on the surface of Fe_3O_4 (Chambers & Joyce, 1999). Surface-sensitive spin polarization measurements made with ultraviolet photoelectron spectroscopy averaging over the entire Brillouin zone measure a spin polarization of −30% to −40% (Tobin et al., 2007). Taking into account the magnetic dead layer results in a bulk spin polarization of −65%, which is close to the predicted −66% photoelectron spin polarization for Fe_3O_4. Prior spin-polarized UPS measurements of Fe_3O_4 measured a spin polarization of −80% for the (111) surface (Dedkov, Rudiger, & Guntherodt, 2002) and −55% for the (001) surface (Fonin, Dedkov,

Pentcheva, Rudiger, & Guntherodt, 2007); these measurements, however, were not averaged over the entire Brillouin zone and are susceptible to band effects.

6.3.2 Strain effects

6.3.2.1 Strain effects in perovskites

Manganites

The application of epitaxial strain through the choice of substrate is another tool used to control the structure and properties of oxide materials. In manganite films, epitaxial strain plays an important role in controlling the magnetic and transport properties. For fully strained $La_{0.7}Sr_{0.3}MnO_3/LaAlO_3$ heterostructures, (110)-oriented films have strongly enhanced transport properties for thicknesses between 3 and 12 nm compared to (001)-oriented films (Tebano, Orsini, Di Castro, Medaglia, & Balestrino, 2010). This effect originates from a reduced tetragonal distortion induced by epitaxy on the (110)-oriented substrates that quenches the occupational imbalance between the Mn e_g orbitals and reinforces the ferromagnetic double exchange transport mechanism.

The effect of biaxial strain on the transport (Figure 6.4(a)) and magnetic (Figure 6.4(b)) properties of $La_{0.7}Sr_{0.3}MnO_3$ (001) films was investigated by varying the biaxial strain from −2.3% to +3.2% (Adamo et al., 2009). In the case of films with a small amount of strain ($|\varepsilon_{xx}| \leq 0.6\%$, i.e., $SrTiO_3$, $(LaAlO_3)_{0.3}$-$(Sr_2AlTaO_6)_{0.7}$ (LSAT), $NdGaO_3$) (Adamo et al., 2009), the low-temperature resistivity values are comparable to single crystals (Shiozaki, Takenaka, Sawaki, & Sugai, 2001). The T_{MI} is higher than 390 K for films under small compressive strain ($NdGaO_3$, $\varepsilon_{xx} = -0.5\%$ and LSAT, $\varepsilon_{xx} = -0.4\%$), whereas T_{MI} is ∼370 K for films under small tensile strains ($SrTiO_3$, $\varepsilon_{xx} = +0.6\%$). Further increasing the tensile strain ($DyScO_3$, $\varepsilon_{xx} = +1.6\%$) results in a decrease in T_{MI} and in the case of large compressive strain ($LaAlO_3$, $\varepsilon_{xx} = -2.3\%$), the films exhibit insulating behavior over the entire temperature range. Large tensile strains (>2.3%) gave rise to films with relatively high resistivity.

An analytical model has been proposed to describe the effects of biaxial strain (ε_{xx} and ε_{yy}) on the magnetotransport properties of the colossal magnetoresistance (MR) manganites (Millis, Darling, & Migliori, 1998). In this model, T_C depends on two parameters: (1) the bulk compression $\varepsilon_B = \frac{1}{3}(2\varepsilon_{xx} + \varepsilon_{zz})$ (assuming $\varepsilon_{xx} = \varepsilon_{yy}$), and (2) the biaxial distortion $\varepsilon^* = 1/2(\varepsilon_{zz} - \varepsilon_{xx})$, where $\varepsilon_{xx} = (a_{xx} - a_{bulk})/a_{bulk}$ and $\varepsilon_{zz} = (a_{zz} - a_{bulk})/a_{bulk}$ are the pseudocubic in-plane and out-of-plane strain, respectively. Uniform compressive (tensile) strain will tend to increase (decrease) the electron-hopping probability, reducing the effect of the electron-lattice coupling; therefore, depending on the sign of the strain, the change in T_C associated with ε_B will be positive or negative, respectively. Conversely, biaxial distortion will only cause a decrease in T_C through an increase in the Jahn−Teller splitting of the e_g electron levels. The effects of strain on the Curie temperature can then be described by the formula $T_C\ (\varepsilon_B, \varepsilon^*) = T_C(0,0)[1 - \alpha\varepsilon_B - b\varepsilon^{*2}]$, where $\alpha = (1/T_C)[(dT_C)/(d\varepsilon_B)]$ and $b = (1/T_c)\ [(d^2T_c)/(d^2\varepsilon^{*2})]$. The T_C behavior of $La_{0.7}Sr_{0.3}MnO_3$ films as a function of ε_B and ε^* (Figure 6.4(c)) has been reported (Adamo et al., 2009), and the measured

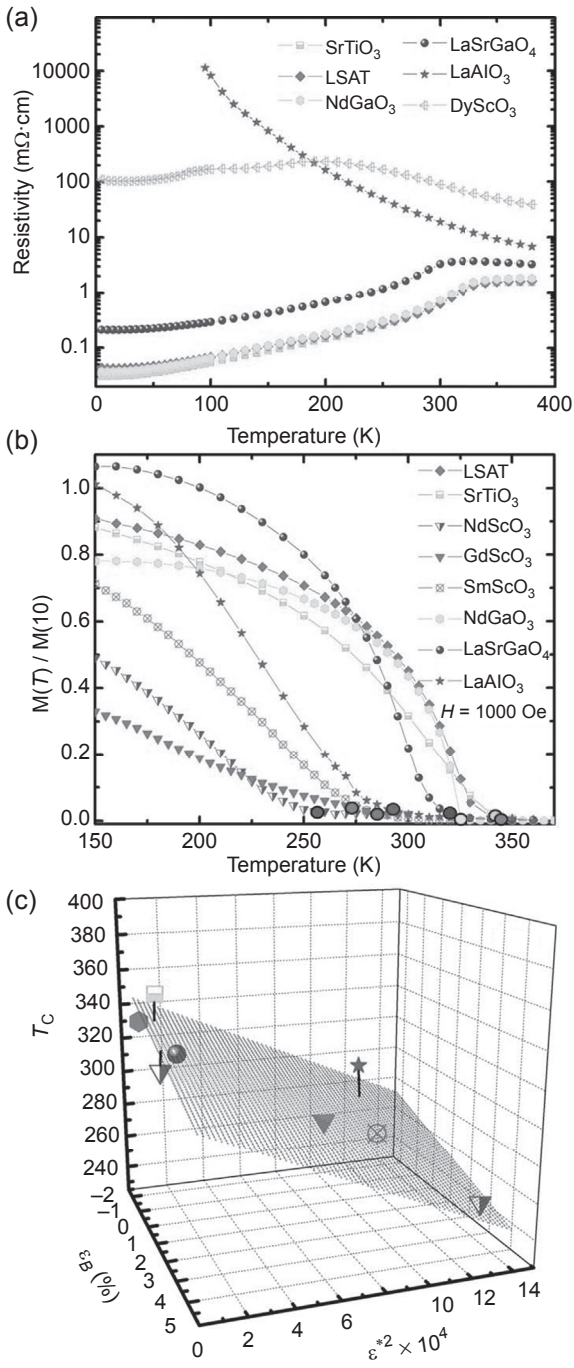

Figure 6.4 (a) Resistivity as a function of temperature for $La_{0.7}Sr_{0.3}MnO_3$ films on different substrates. All films are 22 nm thick, except for that on $NdScO_3$ (10 nm thick film). (b) Field-cooled magnetization as a function of temperature (measured at 1000 Oe) normalized at 10 K, where T_C is denoted by the solid circles. (c) T_C as a function of ε_B and ε^* strains overlaid with the best fit plane to the data. From Adamo et al. (2009).

$T_C(0,0) = 345 \pm 9$ K, $\alpha = 1.55 \pm 0.01$, and $b = 1460 \pm 30$ are in good agreement with theoretical predictions (Millis et al., 1998). Even though there was considerable disagreement on the values of α and b within the literature on $La_{0.7}Sr_{0.3}MnO_3$ films, the authors suggested that the difference arises due to measurements on samples with different thicknesses, which resulted in different and often inhomogeneous strain conditions due to progressive strain relaxation, and using of a smaller number of substrate materials in comparison with their studies (Millis et al., 1998).

Charge-ordered manganites

The charge-ordered phenomena observed in the manganites are also sensitive to epitaxial strain. For tensile-strained $Pr_{0.5}Ca_{0.5}MnO_3/SrTiO_3$ (001) heterostructures, the insulator-to-metal transition below 240 K is induced by applying a 7 T magnetic field (Prellier et al., 2000), which is much lower than the field required in bulk ($\sim$20 T). Electron diffraction studies reveal that films grown on $SrTiO_3$ have significantly increased in-plane Mn−Mn distances (a and c parameters) and Mn−O−Mn angles corresponding to the basic frame of the MnO_6 octahedra (roughly parallel to the substrate). The latter tends toward 180° instead of 150° for the bulk. Consequently, the in-plane metallic conductivity is considerably favored due to the increase of bandwidth. In the case of compressive-strained $Pr_{0.5}Ca_{0.5}MnO_3/LaAlO_3$ (001) heterostructures (Haghiri-Gosnet, Hervieu, Simon, Mercey, & Raveau, 2000), films grow (101)-oriented and electron diffraction studies reveal a monoclinic distortion. Contrary to the bulk, where there is an abrupt increase of $d_{101} (= d_{10\bar{1}})$ and a coupled abrupt decrease of the b parameter at low temperature, the films reveal smooth and small changes. Based on this, the charge-ordering distortion cannot fully develop at low temperature for compressively strained $Pr_{0.5}Ca_{0.5}MnO_3$ films. As a consequence, the charge-exchange antiferromagnetism cannot be obtained, and instead, an insulating-ferromagnetic phase was found with a critical temperature of 240 K.

Nickelates

Stabilization of the perovskite structure with Ni^{3+} can be difficult, but is readily achieved in thin films through a combination of the effect of the perovskite substrate template and the formation of ions with high kinetic energy in the plasma plume during pulsed laser deposition (Catalan, 2008). Epitaxial strain can have large effects on the metal−insulator and magnetic transitions in the nickelates. Compressive strain is accommodated by the film through either a bigger buckling of the oxygen octahedra (which would increase T_{MI}) or shrinking the Ni−O bond distance and therefore a straightening of the buckling angle (which would decrease T_{MI}). It has been suggested that compressive strain should decrease T_{MI} since the Ni−O bond is more compressible than the R−O distance (Catalan, 2008). It has been observed, however, that T_{MI} can decrease for both compressive and tensile strain (Catalan, 2008; Catalan, Bowman, & Gregg, 2000a,b; DeNatale & Kobrin, 1995; Novojilov et al., 2000; Scherwitzl et al., 2010). In bulk, both external hydrostatic pressure (akin to compressive strain) and negative internal chemical pressure (analogous to tensile strain) are known to lower the metal−insulator transition temperature (Catalan, 2008). In both cases, a straightening

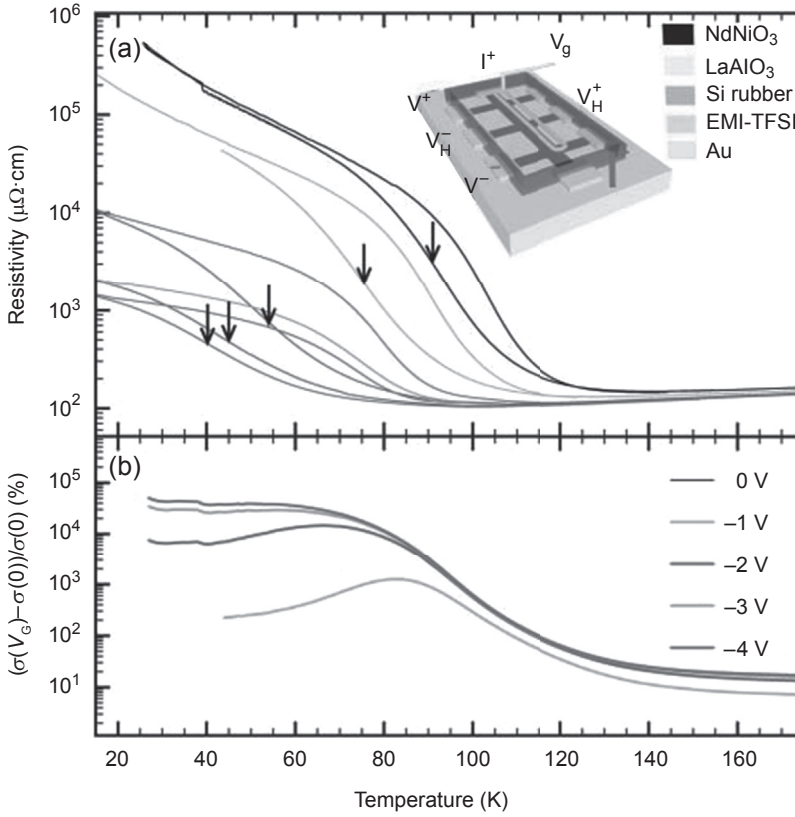

Figure 6.5 (a) The effect of an applied electric field on the resistivity of an 8 u.c. $NdNiO_3/LaAlO_3$ (001) thin film. (b) Electro-conductivity for the same sample and applied voltages as in (a).
From Scherwitzl et al. (2010).

of the Ni−O−Ni bond angle occurs either by a decrease in the Ni−O distance under compressive strain or by an increase in the *R*−O distance under tensile strain. The ability to control the metal−insulator transition in $NdNiO_3$ films with an external electric field was demonstrated (Figure 6.5) (Scherwitzl et al., 2010), which presents an important step toward realizing devices based on electrically controllable phase transitions.

Cobaltites

$LaCoO_3$ is a zero-spin, nonmagnetic material in the bulk, but turns into a ferromagnet below ∼80 K in thin-film form (Choi et al., 2012; Sterbinsky et al., 2012). Utilizing scanning transmission electron microscopy complemented by X-ray and optical spectroscopy, an unconventional strain relaxation behavior resulting in stripe-like, lattice-modulated patterns in $LaCoO_3$ thin films under different strain states has been observed (Choi et al., 2012). This microscopic structural modulation was

reported to strongly couple to the unusual macroscopic ferromagnetic ordering in the $LaCoO_3$ films, with the formation of ferromagnetically ordered sheets comprising intermediate or high-spin Co^{3+}. $LaCoO_3$ films grown under tensile strain revealed stripes running perpendicularly to the surface, which increase in frequency as the tensile strain increased and eventually formed a fairly regular superstructure; these films exhibit a ferromagnetic transition with $T_C = \sim 80$ K. $LaCoO_3$ films grown under slight compressive strain revealed only a few in-plane stripes and did not show any discernible magnetic transition or hysteresis loop. The atomic and electronic structures of $LaCoO_3$ films have also been probed using extended X-ray absorption fine structure spectroscopy in an attempt to further understand the origin of their ferromagnetism (Sterbinsky et al., 2012). These studies revealed a large difference between in-plane and out-of-plane Co−O bond lengths, resulting from the tetragonal distortion in the highly strained films. Based on X-ray absorption near edge spectroscopy, it was suggested that the structural distortions are strongly coupled to the hybridization between the atomic orbitals of Co^{3+} and O^{2-}, but this increased hybridization is not the cause of ferromagnetism. Instead, the strain-induced distortions of the oxygen octahedra increase the population of e_g electrons and concurrently depopulate the t_{2g} electrons beyond a stabilization threshold for ferromagnetic order.

6.3.2.2 Control of magnetic easy axes through strain

Epitaxial strain can also be used to control a material's magnetic easy axis. $La_{0.7}Sr_{0.3}MnO_3$ films grown under compressive and tensile strain possess a magnetic easy axis out-of-plane or in-the-plane of the film, respectively (Kwon et al., 1997). Such effects are seen even in more complex materials such as the multiferroic $BiFeO_3$ (Chu et al., 2007; Martin et al., 2008; Martin & Ramesh, 2012), where strain can tune the nature of the easy axis of magnetization (Holcomb et al., 2010). Through a careful experimental and theoretical study of photoemission electron microscopy (PEEM) images and the underlying structure of $BiFeO_3$, the authors reported that epitaxially strained thin films do not show a degenerate magnetic plane as predicted for bulk, but instead exhibit the formation of a preferred magnetic axis depending on the nature of strain ([112] or $[1\bar{1}0]$ for compressive and tensile strain, respectively) (Holcomb et al., 2010). For compressive strain, for example, the easy axis points as far out of the surface plane as possible while remaining perpendicular to the polarization direction. Thick films no longer retain this preferred direction, instead showing a variation in the magnetic direction, consistent with the perpendicular easy plane behavior observed in bulk (Figure 6.6). These observations enabled a deeper understanding of the magnetic exchange interactions at an interface between such epitaxial $BiFeO_3$ films and a ferromagnet and aid in the design of next-generation devices (Chu et al., 2008).

6.3.2.3 Magnetic anisotropy of $CoFe_2O_4$

Due to the large cubic magnetocrystalline anisotropy, K_1, and magnetostriction, λ_s, constants of $CoFe_2O_4$, the majority of work on understanding strain effects on the

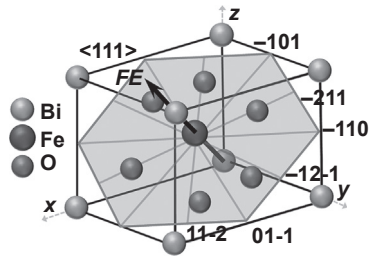

Figure 6.6 Predicted easy magnetic plane (shown as hexagon) for bulk $BiFeO_3$ for a polarization lying along the <111> crystal axis.
Adapted from Holcomb et al. (2010).

spinel ferrites focuses on this material (Slick, 1980). The large K_1 arises from a spin-orbit stabilized doublet ground state of the d^7 electronic configuration of the Co^{2+} cations, which is caused by a trigonal crystal field of the Co^{2+} cations (Dionne, 2009; Slonczewski, 1958a,b; Tachiki, 1960) and has resulted in $CoFe_2O_4$ being included in a number of strain-driven multiferroic devices (Park et al., 2010; Zavaliche et al., 2005; Zhang, Deng, Ma, Lin, & Nan, 2008; Zheng et al., 2004). The magnetic anisotropy of $CoFe_2O_4$/MgO (001) heterostructures is understood by comparing the relative strengths of the magnetoelastic and shape anisotropy energy terms. Coherently strained thin films have an out-of-plane easy axis, as predicted by their large, positive K_1 constant (Chambers et al., 2002; Comes, Gu, Khokhlov, Lu, & Wolf, 2012; Dhakal et al., 2010; Dorsey, Lubitz, Chrisey, & Horwitz, 1996; Lisfi et al., 2007; Moyer, Vaz, Arena et al., 2011). As the film thickness increases and the strain is relaxed, the magnetocrystalline anisotropy contribution is reduced and shape anisotropy dominates, resulting in a reorientation of the easy axes from out-of-plane to in-plane (Lisfi et al., 2007).

The magnetic anisotropy for films grown on $SrTiO_3$ (001) substrates is more complicated than for films grown on MgO due to the large lattice mismatch between $CoFe_2O_4$ and $SrTiO_3$. X-ray diffraction measurements have shown the strain of $CoFe_2O_4$/$SrTiO_3$ (001) heterostructures to be both compressive (Dhakal et al., 2010; Rigato et al., 2009; Xie, Cheng, Wessels, & Dravid, 2008) and tensile (Gao et al., 2009; Moyer, Kumah, Vaz, Arena, & Henrich, 2013); the lattice mismatch suggests that the strain should be compressive. The tensile strain state has been explained by noting that the thermal expansion coefficient is larger for $CoFe_2O_4$ than for $SrTiO_3$, and if the strain relaxes fully during growth, upon cooling the $CoFe_2O_4$ film will have a tensile strain (Gao et al., 2009; Moyer et al., 2013). Independent of whether the strain is compressive or tensile, the magnitude of the strain is larger for films grown on $SrTiO_3$ than for those grown on MgO. This results in larger magnetic anisotropies, with the magnetic easy axis being in-plane (out-of-plane) for films with compressive (tensile) strain. $CoFe_2O_4$ thin films have also been grown on $MgAl_2O_4$, $CoCr_2O_4$-buffered $MgAl_2O_4$, and $CoCr_2O_4$-buffered $SrTiO_3$ (Suzuki, Hu, van Dover, & Cava, 1999). For (001)-oriented substrates, all films are compressively strained and have in-plane easy axes, consistent with the magnetoelastic anisotropy determining the

easy axes. For films grown on (110)-oriented substrates, the easy axis is along the in-plane [100] and the hard axis is along the $[1\bar{1}0]$ (Suzuki et al., 1999). Further annealing of films grown on $CoCr_2O_4$-buffered $MgAl_2O_4$ (110) substrates reorients the easy axis from the [100] direction to the $[1\bar{1}0]$ direction (Hu, Choi, Eom, Harris, & Suzuki, 2000), which is proposed to be due to a reduction in strain energy and a migration of Co^{2+} cations from octahedral to tetrahedral sites.

6.3.2.4 Anisotropic magnetoresistance of Fe_3O_4

Fe_3O_4 has been used as a model system to understand the effects of epitaxial strain and anti-phase boundaries on MR. Before discussing the MR of Fe_3O_4, it is necessary to discuss the Verwey transition. The Verwey transition ($T_V \sim 120$ K) (Verwey, 1939) is a phase transition where the crystal structure changes from cubic to monoclinic and is accompanied by a charge and orbital ordering that results in an increase in the resistivity by over two orders of magnitude (Anderson, 1956; Iizumi et al., 1982; Schrupp et al., 2005). For Fe_3O_4 (001) films grown on MgO and $SrTiO_3$ and Fe_3O_4 (111) grown on Al_2O_3 (0001) substrates, the MR is always negative (Gong, Gupta, Xiao, Qian, & Dravid, 1997; Ogale et al., 1998), with the MR defined as

$$\mathrm{MR} = \frac{\rho_H - \rho_0}{\rho_0}. \tag{6.1}$$

Fe_3O_4 (001) films have an MR that is fairly constant with temperature and on the order of a few percent for temperatures above T_V, a spike in the MR at T_V, and an MR that increases linearly with decreasing temperature below T_V (Gong et al., 1997; Ogale et al., 1998). The MR of Fe_3O_4 (111) at temperatures above T_V increases slowly with decreasing temperature, before increasing linearly below the Verwey transition; there is no sharp spike at T_V, however, as there is for Fe_3O_4 (001) (Ogale et al., 1998). The difference in the size of the MR above T_V between the (001) and (111) films and the absence of a spike in the MR at T_V in the (111) are not understood, but anisotropies exist in both the magnetostriction and the phonon−magnon dispersion, which will affect these films differently due to their different strain states (Ogale et al., 1998). The linear increase in the MR with decreasing temperature below T_V has been attributed to electron transport across anti-phase boundaries (Ziese & Blythe, 2000). MR measurements as a function of magnetic field above T_V show linear and quadratic field dependence for fields applied parallel and perpendicular to the film, respectively (Figure 6.7). This behavior is in agreement with a model of spin-polarized electrons hopping between ferromagnetic chains across an AF interface, demonstrating how anti-phase boundaries dominate the MR (Eerenstein, Palstra, Saxena, et al., 2002).

The MR of Fe_3O_4 is dependent on both the magnetic field and current directions, which is known as anisotropic magnetoresistance (AMR). The AMR for currents along [100] was found to change sign simultaneously with K_1 at a temperature of ~ 150 K (Naftalis et al., 2011; Ziese & Blythe, 2000). In addition, the AMR of Fe_3O_4 cannot be fit to a simple one-band model as in $La_{0.7}Ca_{0.3}MnO_3$, signifying that both minority and

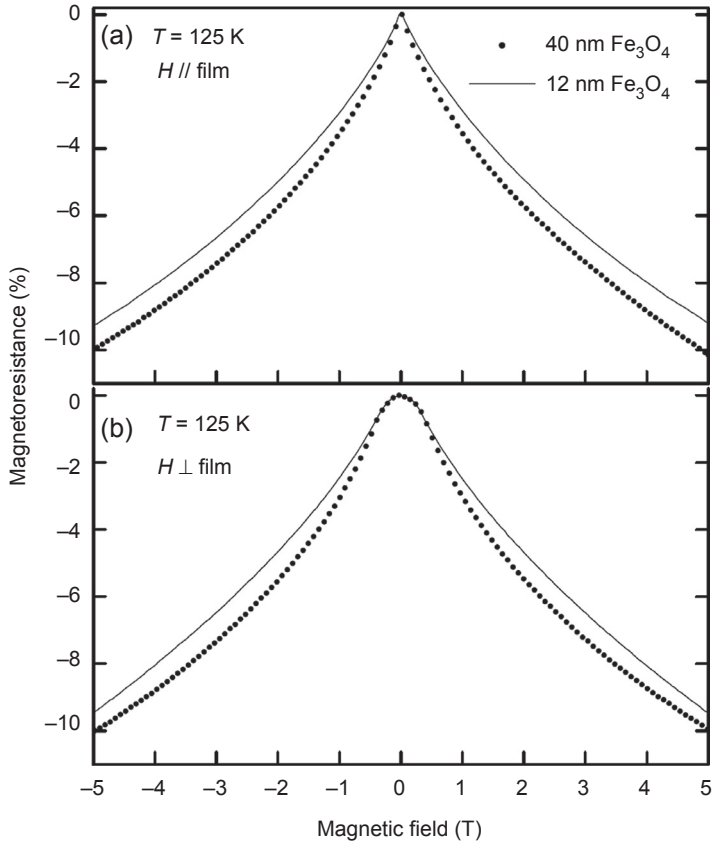

Figure 6.7 Magnetoresistance measured at 125 K for 12 and 40 nm Fe_3O_4 thin films grown on MgO (001) substrates with the magnetic field applied (a) parallel and (b) perpendicular to the film.
From Eerenstein, Palstra, Saxena, et al. (2002).

majority electrons contribute to the conduction in Fe_3O_4; in other words, Fe_3O_4 is not fully spin-polarized (Ziese, 2000). Fe_3O_4/MgO (110) heterostructures show a positive MR when the current and field are parallel to [001] and a negative MR when they are parallel to $[1\bar{1}0]$, in agreement with (001)-oriented films (Sofin, Arora, & Shvets, 2011). The positive MR along [001] is caused by a reduction in the width of the canted spin structure at anti-phase boundaries in this direction since it is the hard axis compared to the $[1\bar{1}0]$ easy axis; at fields above the anisotropy field, the MR becomes negative.

6.3.2.5 *Composite multiferroic structures*

One interesting strain effect studied in depth in recent history is the production of composite (bilayer or nanocomposite) magnetoelectric systems consisting of materials

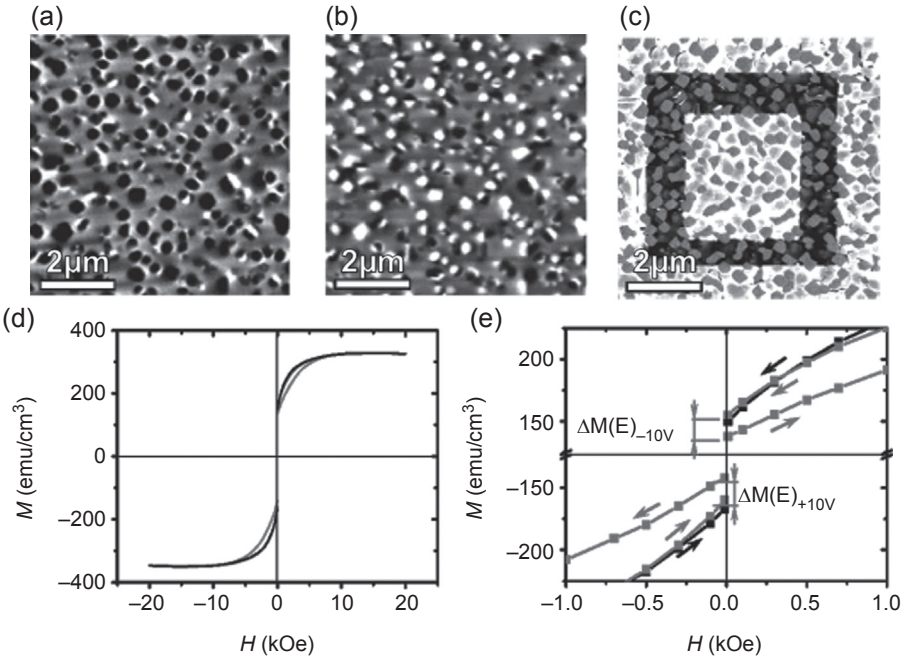

Figure 6.8 (a) Magnetic force microscopy (MFM) image of $(BiFeO_3)_{0.65}$—$(CoFe_2O_4)_{0.35}$ film with the film magnetized perpendicular to the surface with a magnetic field of 20 kOe. (b) MFM image with film magnetized in the opposite direction. (c) Perpendicular piezoelectric force microscopy (PFM) image taken after the film has been poled with −8 V (dark frame), and +8 V (light frame inside box). (d) Magnetization versus field loops measured before (black) and after (gray) electrical polling of 10% of the film area. (e) Zoomed in view of (d).
Adapted from Zavaliche et al. (2005).

with magnetic and ferroelectric/piezoelectric properties. These systems operate by a strain-mediated magnetoelectric coupling between the ferroelectric and magnetic order parameters (Zheng et al., 2004). One example is $BaTiO_3$—$CoFe_2O_4$ self-assembled nanostructures that grow epitaxial both in- and out-of-the-plane to produce arrays of $CoFe_2O_4$ nanopillars embedded in a $BaTiO_3$ matrix. Temperature-dependent magnetic measurements illustrate the coupling between the two order parameters, which is manifested as a change in magnetization at the ferroelectric T_C. Thermodynamic analysis revealed that the magnetoelectric coupling in such a nanostructure can be understood on the basis of the strong elastic interactions between the two phases. Electric field-induced magnetization switching was later demonstrated in the composite $BiFeO_3$—$CoFe_2O_4$ system (Figure 6.8) (Zavaliche et al., 2005). Further, the morphology of self-assembled perovskite-spinel nanostructures can be controlled simply by selecting single-crystal substrates with different orientations (Zheng et al., 2006). For $BiFeO_3$—$CoFe_2O_4$, (001) substrates result in rectangular-shaped $CoFe_2O_4$ nanopillars, whereas (111) substrates result in triangular-shaped $BiFeO_3$ nanopillars.

6.3.3 Interface/multilayer effects

6.3.3.1 $LaMnO_3/SrMnO_3$ superlattices

Advances in the synthesis of complex-oxide heterostructures, with the ability to control unit cell growth and create atomically sharp interfaces, has enabled researchers to achieve collective-ordering phenomena in materials through superlattice and bilayer heterostructures (Catalan et al., 2000b). Superlattices of complex oxides where the superlattice period is below a characteristic length-scale (Scherwitzl et al., 2010) can show unusual collective states (Martin et al., 2008). In the manganites, the superlattice approach has been utilized to synthesis the ordered analogue of $La_{0.74}Sr_{0.26}MnO_3$ by fabricating epitaxial superlattices of $(LaMnO_3)_m(SrMnO_3)_n$ that have a constant stoichiometry of $n/(m+n) = 0.26$ and a superlattice periodicity less than the unit cell distance (Slonczewski, 1958a). This general approach has enabled the study of the effects of strain and cation ordering for a wide range of complex oxides at various doping levels.

In the $La_{1-x}Sr_xMnO_3$ system, electronic, structural, and magnetic transitions occur as the doping level, x, is varied. The parent compounds, $LaMnO_3$ and $SrMnO_3$, are both AF insulators with Mn valence states of 3+ and 4+, respectively. Between $x = 0.15$ and 0.5, charge itinerancy and ferromagnetism are coupled by the double exchange mechanism (Slonczewski, 1958b), which enables electrons to move between neighboring Mn sites when their core t_{2g} spins are aligned in parallel, and forbids this when they are anti-parallel. With increased Sr content ($x > 0.5$), superexchange dominates, and AF order is observed. In addition to altering the Mn valence and magnetic structure, the degree of doping changes the local bonding environment owing to the difference in ionic radii between Sr^{2+}, La^{3+}, and $Mn^{3+/4+}$. In the cubic perovskite structure, Mn^{3+} is in a $3d^4$ ($t_{2g}^3 e_g^1$) state, with a lone electron in the doubly degenerate anti-bonding e_g orbitals ($d_{x^2-y^2}$ and $d_{3z^2-r^2}$). This degeneracy can be removed through tetragonal distortions of the MnO_6 octahedra. The octahedra can also rotate in a cooperative manner in ABO_3 perovskite systems when the A-site cation radius is small enough that $t = \langle A-O\rangle/\sqrt{2}\langle B-O\rangle$ ($\langle A-O\rangle$ and $\langle B-O\rangle$ are the A- and B-site cation-oxygen bond lengths) is less than unity [147]. Distortions or rotations of the MnO_6 octahedra alter the Mn−O−Mn bond angles away from the optimal 180°, reducing the bandwidth for charge transport, which in turn reduces the T_C of double-exchange-mediated ferromagnets. Thus, variance in cation radii can affect local bond angles and tip the balance between competing interactions.

Detailed studies carried out on superlattices composed of the $LaMnO_3$ and $SrMnO_3$ found that $(LaMnO_3)_{2n}/(SrMnO_3)_n$ ($1 \leq n \leq 5$) superlattices undergo a metal−insulator transition (Figure 6.9) as a function of n, being metallic for $n \leq 2$ and insulating for $n \geq 3$ (Bhattacharya et al., 2008). Transport, magnetization, and polarized neutron reflectivity studies revealed the ferromagnetism to be relatively uniform in the metallic state and strongly modulated in the insulating state, being large in $LaMnO_3$ and suppressed in $SrMnO_3$. This modulation is consistent with a Mott transition driven by the proximity between the $(LaMnO_3)/(SrMnO_3)$ interfaces. The insulating state for $n \geq 3$ obeys a variable-range hopping model at low temperatures due to

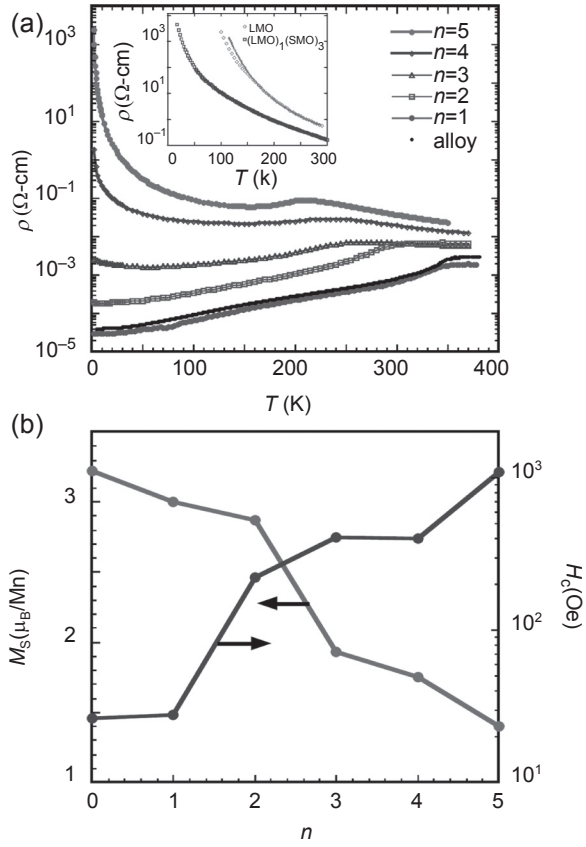

Figure 6.9 (a) Resistivity versus temperature for $La_{0.67}Sr_{0.33}MnO_3$ film and $(SrMnO_3)_n/(LaMnO_3)_{2n}$ superlattices. The inset displays the resistivities for a $LaMnO_3$ thin film and a $(SrMnO_3)_3/(LaMnO_3)_1$ superlattice; the $LaMnO_3$ data are overlaid with a fit to the Arrhenius equation with $E_A = 125$ meV. (b) Change in saturation magnetization (M_S) and coercive field (H_C) with n at $T = 10$ K.
Adapted from Bhattacharya et al. (2008).

states at the Fermi level that emerge at the $(LaMnO_3)/(SrMnO_3)$ interfaces and are localized by disorder. Cation-ordered $(LaMnO_3)_m/(SrMnO_3)_{2m}$ superlattices reveal dramatically enhanced Néel temperatures (T_N), the highest of any $La_{1-x}Sr_xMnO_3$ compound, $\sim$70 K greater than compositionally equivalent randomly doped $La_{1/3}Sr_{2/3}MnO_3$ [142, 148]. The AF order is A-type, consisting of in-plane double-exchange-mediated ferromagnetic sheets coupled antiferromagnetically along the out-of-plane direction. Through synchrotron X-ray scattering, an in-plane structural modulation that reduces the charge itinerancy and hence the ordering temperature within the ferromagnetic sheets, thereby limiting T_N, was noted. This modulation is mitigated and driven to long wavelengths by cation ordering, enabling the higher T_N values of the superlattices. These results provide insight into how cation-site ordering can enhance cooperative behavior in oxides through subtle structural phenomena.

6.3.3.2 Induced ferromagnetism in $LaVO_3/SrVO_3$ superlattices

The discovery of electron conduction at the heteroepitaxial interface of the band insulators $LaAlO_3$ and $SrTiO_3$ (Ohtomo & Hwang, 2004) has resulted in the search for emergent phenomena, such as magnetism, at the interfaces of many other material systems (Hwang et al., 2012). One system in which room-temperature ferromagnetism has been observed is in superlattices of the antiferromagnet $LaVO_3$ ($T_N = 143$ K) and the Pauli paramagnet $SrVO_3$, where one layer of $SrVO_3$ was inserted between two to six layers of $LaVO_3$ ($LaVO_3[m]/SrVO_3$, $m = 2-6$) (Luders, Sheets, David, Prellier, & Fresard, 2009). For an even number of $LaVO_3$ layers, the superlattices are ferromagnetic, whereas for an odd number of $LaVO_3$ layers, the superlattices are nonmagnetic. The magnetic moment for the $m = 6$ superlattice is 1.4 μ_B/V, which is close to the expected value of 1.5 μ_B/V for a $LaVO_3/SrVO_3$ interface, and decreases by only 20% as the temperature increases from 10 to 300 K. Multiple theoretical works have attempted to understand the physics behind the magnetism at this interface, with agreement that octahedral rotations and changes in the charge carrier density at the interface play a role (Dang & Millis, 2013a,b; Schuster, Luders, Fresard, & Schwingenschlogl, 2013). Additionally, there is a predicted alteration of short and long V−O bond lengths along the *c*-axis for odd and even layers of $LaVO_3$ (Schuster et al., 2013). These changes in bond length should give rise to ferromagnetism in an odd number of $LaVO_3$ layers and no magnetism in an even number of $LaVO_3$ layers. While the theoretical prediction for when ferromagnetism should occur disagrees with the experiment, it does predict that there should be changes in the magnetic ordering based on the number of $LaVO_3$ layers.

6.3.3.3 Exchange bias in spinel ferrites

Exchange bias in oxides was first demonstrated with CoO/Fe_3O_4 (001) superlattices grown on NaCl substrates (Terashima & Bando, 1987). By growing CoO/Fe_3O_4 bilayers on $SrTiO_3$ (001) and Al_2O_3 (0001) substrates, the surface orientation can be changed to (001) and (111), respectively (van der Zaag, Ball, Feiner, Wolf, & van der Heijden, 1996). There was no appreciable difference in the exchange bias between the two different surface orientations, both showing an exchange bias field of ~3600 Oe at 5 K. The onset temperature for exchange bias, or blocking temperature (T_B), is dependent on the CoO thickness. For CoO layers above 5 nm, $T_B = 291$ K, which is the Néel temperature of CoO. Below 5 nm, T_B decreases sharply and disappears at 0.4 nm. The exchange bias field (H_{EB}) also depends on the thickness of the CoO, in that it is constant and maximum between 1.6 and 5 nm, before decreasing with increasing thickness and linearly with temperature. The spin structure at the interface of CoO and Fe_3O_4 was examined with neutron diffraction studies of CoO/Fe_3O_4 (001) superlattices grown on MgO (001) (Ijiri et al., 1998). Surprisingly, these measurements showed that the CoO spins are aligned at a 90° angle to the Fe_3O_4 spins. This work demonstrated the need to fully understand the spin alignment of the system in order to accurately model the exchange bias, as most models up to this time had assumed collinear spin alignments. Recently, exchange bias has been demonstrated

in a $Fe_3O_4/BiFeO_3$ bilayer on $SrTiO_3$ (001) (Qu et al., 2012). A maximum $H_{EB} \sim 375$ Oe was measured for a 5-nm $BiFeO_3$ film at 5 K; H_{EB} decreases quickly as both the $BiFeO_3$ thickness and temperature increase, disappearing between 200 and 300 K.

6.3.3.4 Exchange bias in $La_{0.7}Sr_{0.3}MnO_3/BiFeO_3$

An all-perovskite system that shows unique interface coupling and exchange bias is $La_{0.7}Sr_{0.3}MnO_3/BiFeO_3$. By creating an interface between these two materials, a novel ferromagnetic state arises in the antiferromagnet $BiFeO_3$ (Yu et al., 2010). Using X-ray magnetic circular dichroism at the Mn and Fe $L_{2,3}$ edges, the authors discovered that the development of this ferromagnetic spin structure is strongly associated with the onset of a significant exchange bias. Linearly polarized X-ray absorption measurements at the oxygen K edge show that the magnetic state is directly related to an electronic orbital reconstruction at the interface. The ferromagnetic state gives rise to a significant exchange bias interaction with $La_{0.7}Sr_{0.3}MnO_3$, and both exhibit the same temperature dependence. The discovery of correlation between the electronic orbital structure at the interface and exchange bias suggests the possibility of using an electric field to control the magnetization of ferromagnets.

By varying the thickness of the individual layers in $BiFeO_3/La_{0.7}Sr_{0.3}MnO_3$ heterostructures (Huijben et al., 2013), it was found for thick $BiFeO_3$ layers that the exchange bias field is inversely proportional to the thickness of the $La_{0.7}Sr_{0.3}MnO_3$ layers, which is in good agreement with previous studies on conventional exchange bias systems (Nogués & Schuller, 1999). For ultrathin $BiFeO_3$ layers there exists a critical thickness of 2 nm (5 u.c.), below which the exchange bias cannot exist. As previous studies have shown that the ferroelectric polarization remains present in these $BiFeO_3/La_{0.7}Sr_{0.3}MnO_3$ heterostructures down to $BiFeO_3$ thicknesses of only 4 unit cells (Maksymovych et al., 2012), the evolution in the antiferromagnet behavior of the $BiFeO_3$ layer determines the interfacial exchange bias coupling. This was confirmed with linear dichroism X-ray absorption spectroscopy (Figure 6.10), which revealed a strongly reduced linear dichroism for ultrathin $BiFeO_3$ layers.

6.4 Characterization of magnetic-oxide thin films

Characterization of magnetic-oxide thin films includes a range of techniques. The most conventional of these build off of typical measurements applied to bulk materials—including magnetometry (in the form of vibrating sample (VSM) and superconducting quantum interference device (SQUID) magnetometers) and magnetotransport. For magnetometry, the only special consideration that needs to be taken is the relative volume of the magnetic film material as compared to that of the substrate. Because the vastly different volume between a film ($\sim 10^{-7}$–10^{-6} cm^3) and substrate ($\sim 10^{-2}$ cm^3), even a strongly magnetic thin film can be swamped out by the diamagnetic background of the much larger substrate. Additionally, if the substrate includes magnetic ions and a resulting paramagnetic signature (as is the case in rare-earth-containing

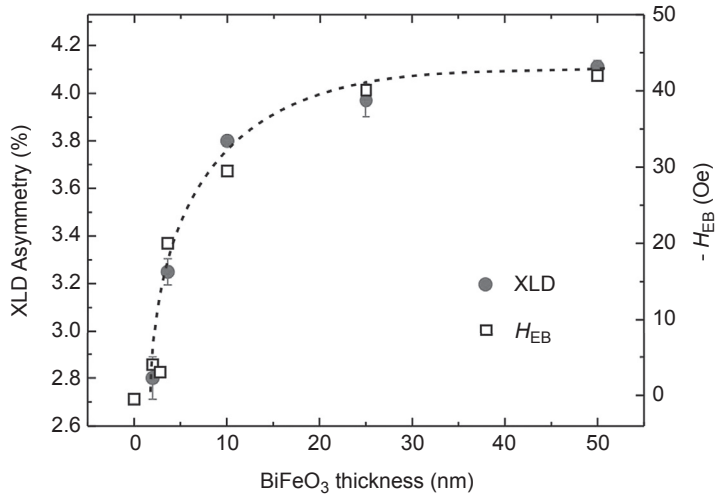

Figure 6.10 Experimental Fe $L_{2,3}$ edge XLD asymmetry (percent of the XAS L_3 peak height signal) and exchange bias shifts (H_{EB}) measured at 17 K as a function of $BiFeO_3$ thickness for $BiFeO_3/La_{0.7}Sr_{0.3}MnO_3$ heterostructures.
From Huijben et al. (2013).

compounds), it might be impossible to measure the film accurately. Finally, for small magnetic moment materials, such approaches might not have the resolution for such small volumes of material and will not be able to resolve the moment accurately. For mangetotransport, the biggest practical challenge corresponds to the magnitude of the resistance of the material. Ultrathin films—even of relative good conductors—can make accurate and stable measurement of the resistance difficult, give rise to drift and noise in magnetotransport measurements, and render resistivity, carrier concentrations, and other values inaccurate.

In such situations, one might need to move to a different probe of magnetic order. For instance, optical probes of magnetism in thin films, including second harmonic generation (Fiebig, Pavlov, & Pisarev, 2005) and magneto-optic Kerr effect (MOKE) (Qiu & Bader, 2000), are easily applied and widely used to sense magnetic response in thin films. The advantage of these techniques comes from their relative simplicity, widespread applicability, and the potential for dynamic study under applied fields. Moving up the scale of complexity, there is growing interest in neutron scattering to probe thin films (Fitzsimmons et al., 2004; Majkrzak, 1996; Saerbeck & Klose, 2012; Schreyer et al., 2000). Such approaches can provide unprecedented access to the nature of magnetic order in materials, but require dedicated time and facilities to accomplish. The last measurement technique we highlight is synchrotron-based probes, including X-ray magnetic linear dichroism (XMLD), circular dichroism (XCMD), and PEEM (He, Arenholz, Scholl, Chu, & Ramesh, 2012; Stöhr, Padmore, Anders, Stammler, & Scheinfein, 1998). Dichroism, or the polarization-dependent absorption of light, provides a way to sensitively probe magnetic order in materials

(Stöhr & Siegmann, 2006). XMCD arises from directional spin alignment (as occurs in ferro- and ferrimagnets) and can be used to measure the size and direction of cation-specific magnetic moments with circularly polarized X-rays. This effect is usually seen at the resonance positions of the magnetic elements. XMLD arises from axial spin alignment (as occurs in ferro-, ferri-, or antiferromagnets) and can be used in the study of antiferromagnetism with linearly polarized X-rays. The axial spin alignment gives rise to a charge distribution anisotropy through spin−orbital coupling, which results in a large XMLD effect typically seen in the absorption fine structure of the resonance peaks of the magnetic elements. Combining XMCD and XMLD measurements and analysis, PEEM imaging has also been widely applied in the study of ferroic materials since it provides a way to spatially map out domain structures in these materials with resolutions as good as 10 nm (Anders et al., 1999).

Modern magnetic thin films, in particular multiferroic materials, can offer challenges to assess magnetic order. Ultimately one might need to call upon multiple measurement techniques to accurately assess the nature of magnetic order. For example, in the candidate multiferroic thin film $PbVO_3$, a combination of SHG and XMLD was used to determine that the material transitioned from a polar 4 mm state to a polar, magnetic state between 100 and 130 K (Figure 6.11). SHG was used to observe a temperature-dependent change in symmetry with the likely onset of a low-temperature G type ($4'/m'mm'$ symmetry) AF phase that, without the combination of techniques, would have not been possible to determine.

6.5 Applications of epitaxial magnetic-oxide thin films

6.5.1 Magnetic tunnel junctions

An MTJ consists of two magnetic layers separated by a thin insulating layer. For magnetic layers that have large spin polarizations, large resistance changes occur through the junction when the moments of the magnetic layers switch from a parallel to an antiparallel alignment. The first observation of MR in an all-oxide MTJ was for a $La_{0.67}Sr_{0.33}MnO_3/SrTiO_3/La_{0.67}Sr_{0.33}MnO_3$ junction, in which an MR of 83% was observed at 4 K (Figure 6.12) (Lu et al., 1996). Further structural improvements to the quality of the heterostructure and the addition of a CoO top pinning layer increased the MR of these MTJs to as high as 1850% at 4 K, corresponding to a spin polarization of 95%, with the MR persisting up to 280 K (Bowen et al., 2003; Sun, KrusinElbaum, Duncombe, Gupta, & Laibowitz, 1997; Viret et al., 1997). Junctions with Fe_3O_4 electrodes separated by MgO have also been fabricated, but they have surprisingly small MR values of 1.5% at 60 K, potentially due to disorder at the interface or formation of $Fe_{1-\delta}O$ (Li, Gupta, Xiao, Qian, & Dravid, 1998). The MR did persist, however, up to 300 K with a value of 0.5%. Lastly, MTJs that use both Fe_3O_4 and LSMO as the magnetic layers have been made with insulating spinel layers, such as $CoCr_2O_4$ (Alldredge, Chopdekar, Nelson-Cheeseman, & Suzuki, 2006; Hu & Suzuki, 2002). The advantage of using different magnetic materials is that the switching fields of the two layers are distinctly separated. These junctions have a maximum MR of −25% at 60 K and

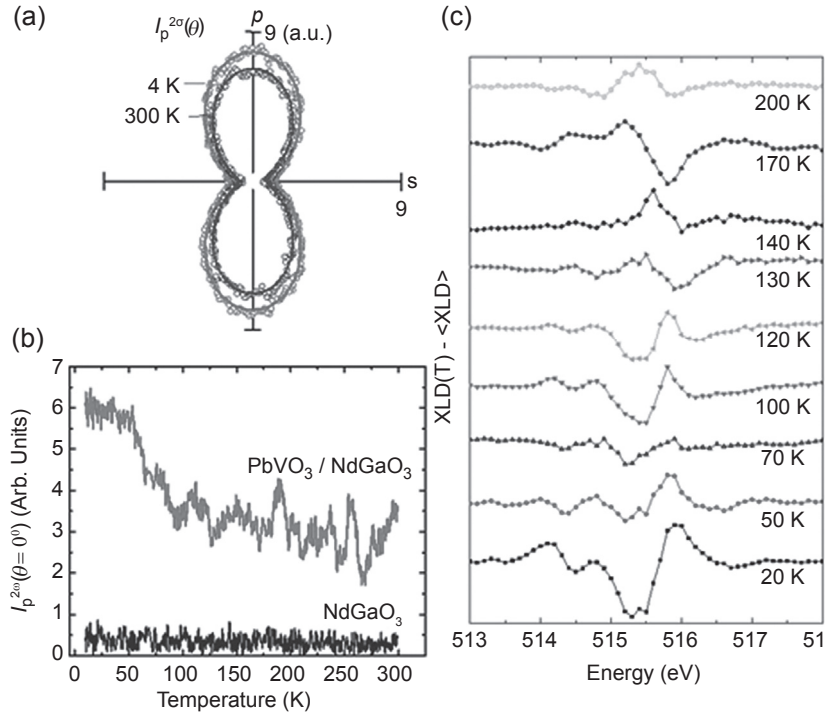

Figure 6.11 (a) SHG intensity of a $PbVO_3/NdGaO_3$ (110) thin-film heterostructure as a function of incoming light angle for a detector fixed at p polarization. (b) Variation of the SHG signal intensity (I_p) at $\theta = 0^\circ$ as a function of temperature revealing a change in SHG signal at around 100 K. (c) X-ray linear dichroism for $PbVO_3/LaAlO_3$ (001) heterostructure as a function of temperature showing the difference between the linear dichroism at a number of given temperatures and the overall average linear dichroism exhibited by the $PbVO_3$ film, again indicating a change in the signal between 120 and 130 K.
Adapted from Kumar et al. (2007).

−0.5% at 300 K, with the negative sign coming from the negative spin polarization of Fe_3O_4 (Hu & Suzuki, 2002).

6.5.2 Spin injection

The efficient injection of spin-polarized electrons into semiconductors is necessary for the development of many proposed spintronic devices (Datta & Das, 1990). The requirements for a material to be a good spin injector are a large spin polarization at the Fermi energy, a small conductivity mismatch with semiconductors, and the ability to be grown epitaxially on common semiconductors. Spin-injection experiments with ferromagnetic metals, such as Fe and Ni, resulted in spin-polarized currents of less than 1% due to a large conductivity mismatch (Schmidt, Ferrand, Molenkamp, Filip, & van Wees, 2000). The spinel ferrites are promising materials to be used as spin injectors

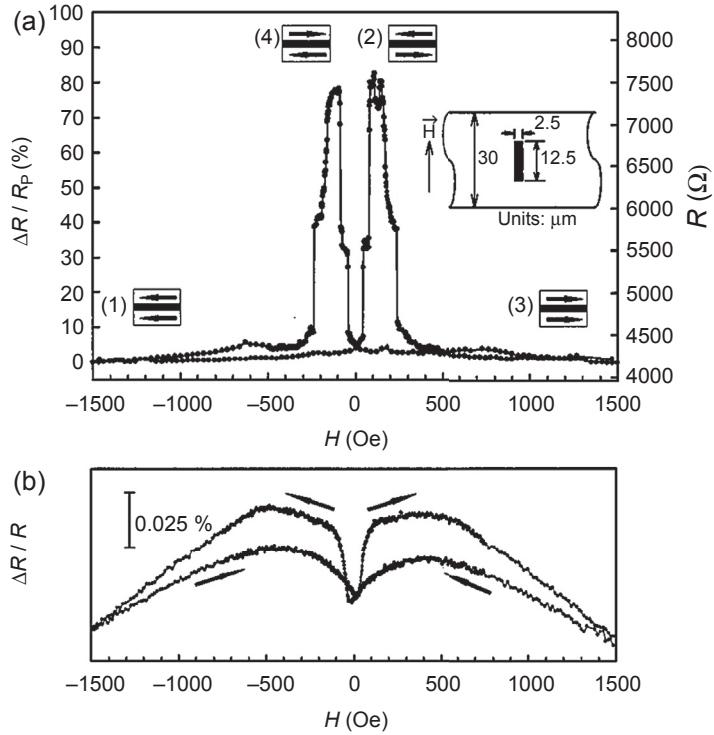

Figure 6.12 (a) Magnetoresistance for an LSMO/$SrTiO_3$/LSMO MTJ measured at 4.2 K. The resistance increases by 84% when the LSMO layers are aligned anti-parallel to each other. (b) MR for the bottom electrode only is less than 1%, demonstrating that the large MR is from the MTJ and not the electrodes themselves.
From Lu et al. (1996).

since they can meet the three requirements listed above. First principle calculations have predicted them to have large spin polarizations (Antonov, Harmon, & Yaresko, 2003; Jeng & Guo, 2002; Szotek et al., 2006; Penicaud, Siberchicot, Sommers, & Kubler, 1992; Zhang & Satpathy, 1991). While Fe_3O_4 has a conductivity larger than semiconductors and other ferrites (MFe_2O_4, M = Mn, Co, Zn) are insulating, alloying Fe_3O_4 with the insulating ferrites enables the conductivity to be tuned by over three orders of magnitude (Ishikawa, Tanaka, & Kawai, 2005; Moyer, Vaz, Negusse, Arena, & Henrich, 2011; Takaobushi et al., 2006; Tripathy, Adeyeye, Boothroyd, & Piramanayagam, 2007; Venkateshvaran et al., 2009). Recently, progress has also been made on growing these materials epitaxially on semiconducting substrates. Spinel ferrites have been grown directly on GaAs (Lu et al., 2005, 2004; Preisler, Brooke, Oldham, & McGill, 2003; Zhang et al., 2011), InAs (Huang et al., 2011), GaN (Zou et al., 2011), and ZnO (Li, Guo, & Bai, 2011), and on Si by using Y_2O_3:ZrO_2 (YSZ) (Bachelet et al., 2011), Sc_2O_3 (Sanchez et al., 2011), and TiN (Kumar, Pandya, & Chaudhary, 2013) buffer layers. A spin polarization of 28% was measured for electrons injected from Fe_3O_4 into ZnO.

6.5.3 Spin filters

Spin-filter devices filter spin-polarized electrons that tunnel between ferromagnetic and nonmagnetic metals through a ferromagnetic insulator. This phenomenon is realized through the different tunneling barrier heights of the insulating magnetic layer for spin up and spin down electrons. $BiMnO_3$ was the first oxide material that was used as a spin filter, where a 50% change in the tunneling resistance of an Au/3.5 nm $BiMnO_3$/1 nm $SrTiO_3$/LSMO/$SrTiO_3$ (001) device was measured at 3 K, corresponding to a spin-filtering efficiency of 22% (Gajek et al., 2005). Since a $T_C = 105$ K for $BiMnO_3$ eliminates the potential for room temperature spin-filtering, the majority of recent research has focused on the spinel ferrites. The spin-filter effect has been observed using $CoFe_2O_4$ (Chapline & Wang, 2006; Ramos et al., 2007; Takahashi et al., 2010), $NiFe_2O_4$ (Luders et al., 2006), and $MnFe_2O_4$ (Matzen, Moussy, Miao, & Moodera, 2013) barrier layers, with $CoFe_2O_4$ having a measured spin filter efficiency of −4% at room temperature (Ramos et al., 2007; Takahashi et al., 2010). Recently, single-domain $CoFe_2O_4$ nanojunctions with a cross-section of ∼5 nm produced a room temperature spin-filter efficiency of −8% (Figure 6.13) (Matzen et al., 2012). These spin-filter efficiencies have been determined from evaluating Jullière's formula (Julliere, 1975) for an MTJ. Measurements of the spin-filter efficiency using superconducting electrodes, however, result in positive spin-filter efficiencies for $CoFe_2O_4$ (Ramos et al., 2008; Rigato et al., 2010), demonstrating how the band alignments between the electrodes and the spin-filtering materials and the wave-function symmetry of the bands can result in a change in sign in the spin-filter efficiency (Caffrey, Fritsch,

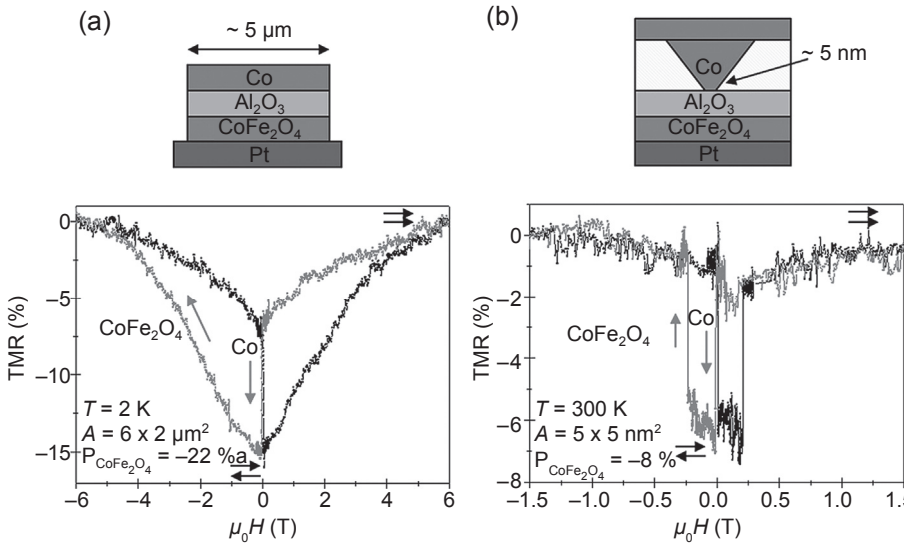

Figure 6.13 Magnetoresistance of (a) 5-μm and (b) 5-nm Co/Al_2O_3/$CoFe_2O_4$/Pt spin-filter junctions. The 5-μm junction has a spin-filter efficiency of −22% at 2 K, while the 5-nm junction has a −8% spin-filter efficiency at 300 K.
From Matzen et al. (2012).

Archer, Sanvito, & Ederer, 2013). It has been proposed that an electric field gate could be used to reversibly change the sign of a spin filter (Caffrey et al., 2013).

6.6 Future of epitaxy of complex-oxide magnets

6.6.1 Frustrated systems

A magnetic material in which all of the pairwise magnetic interactions cannot be simultaneously satisfied is called frustrated. Magnetic frustration is common in bulk materials, exemplified by the spin ice pyrochlores, such as $Dy_2Ti_2O_7$ (Bramwell & Gingras, 2001; Ramirez, Hayashi, Cava, Siddharthan, & Shastry, 1999). Epitaxial thin films provide a unique opportunity for studying and perturbing magnetic frustration, since they enable the opportunity to alter both the symmetry of the system through epitaxial strain and the strength of the magnetic interactions through chemical substitution. While magnetic frustration exists in many oxide systems—such as spinel ferrites and chromates (Iwata et al., 2009; Yamamoto, Tanaka, & Kawai, 2001), hexagonal and perovskite manganites (Fujimura, Takahashi, Yoshimura, & Ashida, 2007; Yang et al., 2006), and double perovskites (Chakraverty et al., 2011)—due to the lack of suitable substrates many of the popular bulk magnetically frustrated materials, like the spin-ice pyrochlores, are just now being investigated as epitaxially strained thin films (Bovo et al., 2014; Leusink et al., 2014).

6.6.2 Flexomagnetism

The flexoelectric effect results in a shift in a ferroelectric hysteresis loop when a strain gradient exists throughout a ferroelectric. This has been demonstrated in thin films by growing a compositionally graded $PbZr_{1-x}Ti_xO_3$, where the strain gradient is created by coherently straining the compositionally graded film to a substrate (Mangalam, Karthik, Damodaran, Agar, & Martin, 2013). The free energy equation for magnetic systems contains an equivalent term for flexomagnetism:

$$F_{\text{flexomagnetism}} = -\nu_{ijkl} H_i \frac{\partial \sigma_{jk}}{\partial x_l}, \tag{6.2}$$

where ν_{ijkl} is the flexomagnetic tensor (Lukashev & Sabirianov, 2010). Since this energy term is linear in H, a strain gradient would result in a shift in the magnetic hysteresis loop. While there has yet to be experimental confirmation of the flexomagnetic effect, theory has predicted its occurrence (Lukashev & Sabirianov, 2010), and epitaxial thin films are a promising avenue for investigating flexomagnetism.

6.6.3 Challenges and summary

Many challenges still exist in the field of epitaxial magnetic oxides, one of which is a lack of substrates. While many substrates exist for the growth of perovskites, other

magnetic systems have relatively few options. Developing new substrates that enable strain-engineered films of spinels, pyrochlores, garnets, etc. will allow for a greater understanding of how strain affects their magnetic properties. Additionally, the production of magnetically inert substrates (by controlling the constituent species or impurities) is essential.

A second challenge is the ability to make accurate measurements on magnetic devices. Many devices require thin films with thicknesses of nanometers and areas of hundreds of microns. The most accurate method to measure magnetism is to use a SQUID magnetometer, but it does not have the sensitivity to measure magnetic devices with these dimensions. A MOKE magnetometer can measure the magnetic properties of devices, but it is not inherently quantitative. Making accurate magnetic measurements on magnetic devices is a challenge, and researchers need to take care when designing devices in order to accurately report the performance of magnetic devices.

Lastly, there is a lot of interest in nonmagnetic materials and superlattices that exhibit magnetism in thin film form. The magnitude of this magnetism is often quite small, on the order of a fraction of a Bohr magneton per cation. In response to reports about magnetism in HfO_2, researchers demonstrated that HfO_2 films are nonmagnetic, but appear to have room temperature ferromagnetism when handled with stainless steel tweezers (Abraham, Frank, & Guha, 2005). This example highlights the care necessary to not magnetically contaminate samples when reporting on the emergence of magnetism in nonmagnetic bulk systems.

In summary, magnetic oxides are a fascinating class of materials to study for both their complex physical nature and their potential use in many novel devices. Epitaxial growth of these materials enables one to control their magnetic properties and spin structures through application of epitaxial strain, control of film thickness, creation of superlattices, and coupling with other ferroic-order parameters. While many challenges still remain, particularly with increasing the temperature limit of these materials to above room temperature, an incredible amount of knowledge has already been attained that has enabled the understanding of many novel phenomena, such as magnetic dead layers, ferromagnetism at the interface of nonferromagnetic oxides, precise control of T_C, exchange bias, the spin-filter effect, etc. With the continued advances in thin-film growth technology and the emerging research in systems such as the magnetoelectric multiferroics, one can only expect numerous new and exciting scientific discoveries in the field of epitaxial magnetic oxides in the near future.

Acknowledgments

The authors acknowledge the support of the National Science Foundation under grant DMR-1149062 and DMR-1124696 as well as support from the Army Research Office under grant W911NF-14-1-0104.

References

Abraham, D. W., Frank, M. M., & Guha, S. (2005). Absence of magnetism in hafnium oxide films. *Applied Physics Letters, 87*, 252502.

Adamo, C., Ke, X., Wang, H. Q., Xin, H. L., Heeg, T., Hawley, M. E., et al. (2009). Effect of biaxial strain on the electrical and magnetic properties of (001) $La_{0.7}Sr_{0.3}MnO_3$ thin films. *Applied Physics Letters, 95*, 112504.

Aizu, K. (1970). Possible species of ferromagnetic, ferroelectric, and ferroelastic crystals. *Physical Review B, 2*, 754.

Alldredge, L. M. B., Chopdekar, R. V., Nelson-Cheeseman, B. B., & Suzuki, Y. (2006). Spin-polarized conduction in oxide magnetic tunnel junctions with magnetic and nonmagnetic insulating barrier layers. *Applied Physics Letters, 89*, 182504.

Alonso, J. A., Martínez-Lope, M. J., Casais, M. T., Aranda, M. A. G., & Fernández-Díaz, M. T. (1999). Metal−Insulator transitions, structural and microstructural evolution of $RNiO_3$ (R = Sm, Eu, Gd, Dy, Ho, Y) Perovskites: evidence for room-temperature charge disproportionation in monoclinic $HoNiO_3$ and $YNiO_3$. *Journal of the American Chemical Society, 121*, 4754.

Anderson, P. W. (1950). Antiferromagnetism − theory of superexchange interaction. *Physical Review, 79*, 350.

Anderson, P. W. (1956). Ordering and antiferromagnetism in ferrites. *Physical Review, 102*, 1008.

Anders, S., Padmore, H. A., Duarte, R. M., Renner, T., Stammler, T., Scholl, A., et al. (1999). Photoemission electron microscope for the study of magnetic materials. *Review of Scientific Instruments, 70*, 3973.

Antonov, V. N., Harmon, B. N., & Yaresko, A. N. (2003). Electronic structure and x-ray magnetic circular dichroism in Fe_3O_4 and Mn-, Co-, or Ni-substituted Fe_3O_4. *Physical Review B, 67*, 024417.

Aydogdu, G. H., Ha, S. D., Viswanath, B., & Ramanathan, S. (2011). Epitaxy, strain, and composition effects on metal-insulator transition characteristics of $SmNiO_3$ thin films. *Journal of Applied Physics, 109*, 124110.

Azuma, M., Takata, K., Saito, T., Ishiwata, S., Shimakawa, Y., & Takano, M. (2005). Designed ferromagnetic, ferroelectric Bi_2NiMnO_6. *Journal of the American Chemical Society, 127*, 8889.

Bachelet, R., de Coux, P., Warot-Fonrose, B., Skumryev, V., Fontcuberta, J., & Sanchez, F. (2011). $CoFe_2O_4$/buffer layer ultrathin heterostructures on Si(001). *Journal of Applied Physics, 110*, 086102.

Bader, S. D. (1990). Thin-film magnetism. *Proceedings of the IEEE, 78*, 909.

Bhattacharya, A., May, S. J., te Velthuis, S. G. E., Warusawithana, M., Zhai, X., Jiang, B., et al. (2008). Metal-insulator transition and its relation to magnetic structure in $(LaMnO_3)_{2n}$/$(SrMnO_3)_n$ superlattices. *Physical Review Letters, 100*, 257203.

Boschker, H., Kautz, J., Houwman, E. P., Siemons, W., Blank, D. H. A., Huijben, M., et al. (2012). High-temperature magnetic insulating phase in ultrathin $La_{0.67}Sr_{0.33}MnO_3$ films. *Physical Review Letters, 109*, 157207.

Bovo, L., Moya, X., Prabhakaran, D., Soh, Y.-A., Boothroyd, A. T., Mathur, N. D., Aeppli, G., & Bramwell, S. T. (2014). Restoration of the third law in spin ice thin films. *Nature Communications, 5*, 3439.

Bowen, M., Bibes, M., Barthelemy, A., Contour, J. P., Anane, A., Lemaitre, Y., et al. (2003). Nearly total spin polarization in $La_{2/3}Sr_{1/3}MnO_3$ from tunneling experiments. *Applied Physics Letters, 82*, 233.

Bramwell, S. T., & Gingras, M. J. P. (2001). Spin ice state in frustrated magnetic pyrochlore materials. *Science, 294*, 1495.

Caffrey, N. M., Fritsch, D., Archer, T., Sanvito, S., & Ederer, C. (2013). Spin-filtering efficiency of ferrimagnetic spinels $CoFe_2O_4$ and $NiFe_2O_4$. *Physical Review B, 87*, 024419.

Catalan, G. (2008). Progress in perovskite nickelate research. *Phase Transitions, 81*, 729.

Catalan, G., Bowman, R. M., & Gregg, J. M. (2000a). Metal-insulator transitions in $NdNiO_3$ thin films. *Physical Review B, 62*, 7892.

Catalan, G., Bowman, R. M., & Gregg, J. M. (2000b). Transport properties of $NdNiO_3$ thin films made by pulsed-laser deposition. *Journal of Applied Physics, 87*, 606.

Catalan, G., & Scott, J. F. (2009). Physics and applications of bismuth ferrite. *Advanced Materials, 21*, 2463.

Celotto, S., Eerenstein, W., & Hibma, T. (2003). Characterization of anti-phase boundaries in epitaxial magnetite films. *European Physical Journal B: Condensed Matter and Complex Systems, 36*, 271.

Chakhalian, J., Rondinelli, J. M., Liu, J., Gray, B. A., Kareev, M., Moon, E. J., et al. (2011). Asymmetric orbital-lattice interactions in ultrathin correlated oxide films. *Physical Review Letters, 107*, 116805.

Chakraverty, S., Saito, M., Tsukimoto, S., Ikuhara, Y., Ohtomo, A., & Kawasaki, M. (2011). Magnetic properties of Sr_2FeTaO_6 double perovskite epitaxially grown by pulsed-laser deposition. *Applied Physics Letters, 99*, 3.

Chambers, S. A., Farrow, R. F. C., Maat, S., Toney, M. F., Folks, L., Catalano, J. G., et al. (2002). Molecular beam epitaxial growth and properties of $CoFe_2O_4$ on MgO(001). *Journal of Magnetism and Magnetic Materials, 246*, 124.

Chambers, S. A., & Joyce, S. A. (1999). Surface termination, composition and reconstruction of Fe_3O_4(001) and γ-Fe_2O_3(001). *Surface Science, 420*, 111.

Chapline, M. G., & Wang, S. X. (2006). Room-temperature spin filtering in a $CoFe_2O_4$/MgAl2O4/Fe_3O_4 magnetic tunnel barrier. *Physical Review B, 74*, 014418.

Cheong, S.-W., & Mostovoy, M. (2007). Multiferroics: a magnetic twist for ferroelectricity. *Nature Materials, 6*, 13.

Choi, J., Eom, C. B., Rijnders, G., Rogalla, H., & Blank, D. H. A. (2001). Growth mode transition from layer by layer to step flow during the growth of heteroepitaxial $SrRuO_3$ on (001) $SrTiO_3$. *Applied Physics Letters, 79*, 1447.

Choi, W. S., Kwon, J.-H., Jeen, H., Hamann-Borrero, J. E., Radi, A., Macke, S., et al. (2012). Strain-induced spin states in atomically ordered cobaltites. *Nano Letters, 12*, 4966.

Chu, Y.-H., Martin, L. W., Holcomb, M. B., Gajek, M., Han, S.-J., He, Q., et al. (2008). Electric-field control of local ferromagnetism using a magnetoelectric multiferroic. *Nature Materials, 7*, 478.

Chu, Y.-H., Martin, L. W., Holcomb, M. B., & Ramesh, R. (2007). Controlling magnetism with multiferroics. *Materials Today, 10*, 16.

Coey, J. M. D., Venkatesan, M., & Xu, H. (2013). Introduction to magnetic oxides. In S. B. Ogale, T. V. Venkatesan, & M. Blamire (Eds.), *Functional metal oxides: New science and novel applications* (p. 1). Weinheim: Wiley-VCH Verlag GmbH & Co. KGaA.

Coey, J. M. D., Viret, M., & von Molnár, S. (1999). Mixed-valence manganites. *Advances in Physics, 48*, 167.

Comes, R., Gu, M., Khokhlov, M., Lu, J. W., & Wolf, S. A. (2012). Microstructural and domain effects in epitaxial $CoFe_2O_4$ films on MgO with perpendicular magnetic anisotropy. *Journal of Magnetism and Magnetic Materials, 324*, 524.

Conchon, F., Boulle, A., Guinebretière, R., Girardot, C., Pignard, S., Kreisel, J., et al. (2007). Effect of tensile and compressive strains on the transport properties of $SmNiO_3$ layers epitaxially grown on (001) $SrTiO_3$ and $LaAlO_3$ substrates. *Applied Physics Letters, 91*, 192110.

Dagotto, E. (2003). *Nanoscale phase separation and colossal magnetoresistance: The physics of manganites and related compounds*. Berlin: Springer.

Dagotto, E. (2005). Complexity in strongly correlated electronic systems. *Science, 309*, 257.

Dang, H. T., & Millis, A. J. (2013). Designing ferromagnetism in vanadium oxide based superlattices. *Physical Review B, 87*, 184434.

Dang, H. T., & Millis, A. J. (2013). Theory of ferromagnetism in vanadium-oxide based perovskites. *Physical Review B, 87*, 155127.

Das, H., Wysocki, A. L., Geng, Y., Wu, W., & Fennie, C. J. (2014). Bulk magnetoelectricity in the hexagonal manganites and ferrites. *Nature Communications, 5*, 2998.

Datta, S., & Das, B. (1990). Electronic analog of the electrooptic modulator. *Applied Physics Letters, 56*, 665.

Dedkov, Y. S., Rudiger, U., & Guntherodt, G. (2002). Evidence for the half-metallic ferromagnetic state of Fe_3O_4 by spin-resolved photoelectron spectroscopy. *Physical Review B, 65*, 064417.

DeNatale, J. F., & Kobrin, P. H. (1995). Lattice distortion effects on electrical switching in epitaxial thin film $NdNiO_3$. *Journal of Materials Research, 10*, 2992.

Dhakal, T., Mukherjee, D., Hyde, R., Mukherjee, P., Phan, M. H., Srikanth, H., et al. (2010). Magnetic anisotropy and field switching in cobalt ferrite thin films deposited by pulsed laser ablation. *Journal of Applied Physics, 107*, 053914.

Dionne, G. F. (2009). *Magnetic oxides*. Boston: Springer Science+Business Media, LLC.

Disa, A. S., Kumah, D. P., Ngai, J. H., Specht, E. D., Arena, D. A., Walker, F. J., et al. (2013). Phase diagram of compressively strained nickelate thin films. *APL Materials, 1*, 032110.

Dorsey, P. C., Lubitz, P., Chrisey, D. B., & Horwitz, J. S. (1996). $CoFe_2O_4$ thin films grown on (100)MgO substrates using pulsed laser deposition. *Journal of Applied Physics, 79*, 6338.

Dzyaloshinskii, I. E. (1957). Thermodynamic theory of weak ferromagnetism in antiferromagnetic substances. *Soviet Physics JETP, 5*, 1259.

Eerenstein, W., Hibma, T., & Celotto, S. (2004). Mechanism for superparamagnetic behavior in epitaxial Fe_3O_4 films. *Physical Review B, 70*, 6.

Eerenstein, W., Mathur, N. D., & Scott, J. F. (2006). Multiferroic and magnetoelectric materials. *Nature, 442*, 759.

Eerenstein, W., Palstra, T. T. M., Hibma, T., & Celotto, S. (2002). Origin of the increased resistivity in epitaxial Fe_3O_4 films. *Physical Review B, 66*, 201101R.

Eerenstein, W., Palstra, T. T. M., Saxena, S. S., & Hibma, T. (2002). Spin-polarized transport across sharp antiferromagnetic boundaries. *Physical Review Letters, 88*, 247204.

Eguchi, R., Okamoto, Y., Hiroi, Z., Shin, S., Chainani, A., Tanaka, Y., et al. (2009). Structure and photoemission spectroscopy of strain-controlled metal-insulator transition in $NdNiO_3$ thin films. *Journal of Applied Physics, 105*, 056103.

Eom, C. B. (1997). Epitaxial thin films of isotropic conductive oxides for devices. *JOM, 49*, 47.

Fiebig, M., Lottermoser, T., Frohlich, D., Goltsev, A. V., & Pisarev, R. V. (2002). Observation of coupled magnetic and electric domains. *Nature, 419*, 818.

Fiebig, M., Pavlov, V. V., & Pisarev, R. V. (2005). Second-harmonic generation as a tool for studying electronic and magnetic structures of crystals: review. *Journal of the Optical Society of America B, 22*, 96.

Fischer, P., Polomska, M., Sosnowska, I., & Szymanski, M. (1980). Temperature dependence of the crystal and magnetic structures of $BiFeO_3$. *Journal of Physics C: Solid State Physics, 13*, 1931.

Fitzsimmons, M. R., Bader, S. D., Borchers, J. A., Felcher, G. P., Furdyna, J. K., Hoffmann, A., et al. (2004). Neutron scattering studies of nanomagnetism and artificially structured materials. *Journal of Magnetism and Magnetic Materials, 271*, 103.

Fonin, M., Dedkov, Y. S., Pentcheva, R., Rudiger, U., & Guntherodt, G. (2007). Magnetite: a search for the half-metallic state. *Journal of Physics: Condensed Matter, 19*, 315217.

Fujimura, N., Takahashi, T., Yoshimura, T., & Ashida, A. (2007). Magnetic frustration behavior of ferroelectric ferromagnet $YbMnO_3$ epitaxial films. *Journal of Applied Physics, 101*, 09M107.

Gajek, M., Bibes, M., Barthelemy, A., Bouzehouane, K., Fusil, S., Varela, M., et al. (2005). Spin filtering through ferromagnetic $BiMnO_3$ tunnel barriers. *Physical Review B, 72*, 020406.

Gajek, M., Bibes, M., Fusil, S., Bouzehouane, K., Fontcuberta, J., Barthelemy, A., et al. (2007). Tunnel junctions with multiferroic barriers. *Nature Materials, 6*, 296.

Gao, X. S., Bao, D. H., Birajdar, B., Habisreuther, T., Mattheis, R., Schubert, M. A., et al. (2009). Switching of magnetic anisotropy in epitaxial $CoFe_2O_4$ thin films induced by $SrRuO_3$ buffer layer. *Journal of Physics D: Applied Physics, 42*, 175006.

Gao, Y., Kim, Y. J., & Chambers, S. A. (1998). Preparation and characterization of epitaxial iron oxide films. *Journal of Materials Research, 13*, 2003.

Gélard, I., Jehanathan, N., Roussel, H., Gariglio, S., Lebedev, O. I., Van Tendeloo, G., et al. (2011). Off-stoichiometry effects on the crystalline and defect structure of hexagonal manganite $REMnO_3$ films (RE = V, Er, Dy). *Chemistry of Materials, 23*, 1232.

Gong, G. Q., Gupta, A., Xiao, G., Qian, W., & Dravid, V. P. (1997). Magnetoresistance and magnetic properties of epitaxial magnetite thin films. *Physical Review B, 56*, 5096.

Haghiri-Gosnet, A. M., Hervieu, M., Simon, C., Mercey, B., & Raveau, B. (2000). Charge ordering in $Pr_{0.5}Ca_{0.5}MnO_3$ thin films: a new form initiated by strain effects of $LaAlO_3$ substrate. *Journal of Applied Physics, 88*, 3545.

Haghiri-Gosnet, A. M., & Renard, J. P. (2003). CMR manganites: physics, thin films and devices. *Journal of Physics D: Applied Physics, 36*, R127.

Han, J. W., & Yildiz, B. (2011). Enhanced one dimensional mobility of oxygen on strained $LaCoO_3$(001) surface. *Journal of Materials Chemistry, 21*, 18983.

He, Q., Arenholz, E., Scholl, A., Chu, Y. H., & Ramesh, R. (2012). Nanoscale characterization of emergent phenomena in multiferroics. *Current Opinion in Solid State & Materials Science, 16*, 216.

Hill, N. A., Battig, P., & Daul, C. (2002). First principles search for multiferroism in $BiCrO_3$. *Journal of Physical Chemistry B, 106*, 3383.

Holcomb, M. B., Martin, L. W., Scholl, A., He, Q., Yu, P., Yang, C. H., et al. (2010). Probing the evolution of antiferromagnetism in multiferroics. *Physical Review B, 81*, 134406.

Hong, W., Lee, H. N., Yoon, M., Christen, H. M., Lowndes, D. H., Suo, Z., et al. (2005). Persistent step-flow growth of strained films on vicinal substrates. *Physical Review Letters, 95*, 095501.

Huang, Z. C., Zhai, Y., Xu, Y. B., Wu, J., Thompson, S. M., & Holmes, S. N. (2011). Growth and magnetic properties of ultrathin single crystal Fe_3O_4 film on InAs(100). *Physica Status Solidi A: Applications and Materials Science, 208*, 2377.

Hu, G., Choi, J. H., Eom, C. B., Harris, V. G., & Suzuki, Y. (2000). Structural tuning of the magnetic behavior in spinel-structure ferrite thin films. *Physical Review B, 62*, R779.

Huijben, M., Martin, L. W., Chu, Y. H., Holcomb, M. B., Yu, P., Rijnders, G., et al. (2008). Critical thickness and orbital ordering in ultrathin $La_{0.7}Sr_{0.3}MnO_3$ films. *Physical Review B, 78*, 094413.

Huijben, M., Yu, P., Martin, L. W., Molegraaf, H. J. A., Chu, Y. H., Holcomb, M. B., et al. (2013). Ultrathin limit of exchange bias coupling at oxide multiferroic/ferromagnetic interfaces. *Advanced Materials, 25*, 4739.

Hu, G., & Suzuki, Y. (2002). Negative spin polarization of Fe_3O_4 in magnetite/manganite-based junctions. *Physical Review Letters, 89*, 276601.

Hwang, H. Y., Iwasa, Y., Kawasaki, M., Keimer, B., Nagaosa, N., & Tokura, Y. (2012). Emergent phenomena at oxide interfaces. *Nature Materials, 11*, 103.

Iizumi, M., Koetzle, T. F., Shirane, G., Chikazumi, S., Matsui, M., & Todo, S. (1982). Structure of magnetite (Fe_3O_4)below the Verwey transition temperature. *Acta Crystallography B, 38*, 2121.

Ijiri, Y., Borchers, J. A., Erwin, R. W., Lee, S. H., van der Zaag, P. J., & Wolf, R. M. (1998). Perpendicular coupling in exchange-biased Fe_3O_4/CoO superlattices. *Physical Review Letters, 80*, 608.

Ishikawa, M., Tanaka, H., & Kawai, T. (2005). Preparation of highly conductive Mn-doped Fe_3O_4 thin films with spin polarization at room temperature using a pulsed-laser deposition technique. *Applied Physics Letters, 86*, 222504.

Iwata, J. M., Chopdekar, R. V., Wong, F. J., Nelson-Cheeseman, B. B., Arenholz, E., & Suzuki, Y. (2009). Enhanced magnetization of $CuCr_2O_4$ thin films by substrate-induced strain. *Journal of Applied Physics, 105*, 3.

Jeng, H.-T., & Guo, G. Y. (2002). First-principles investigations of the magnetocrystalline anisotropy in strained Co-substituted magnetite ($CoFe_2O_4$). *Journal of Magnetism and Magnetic Materials, 239*, 88.

Jonker, G. H., & Van Santen, J. H. (1950). Ferromagnetic compounds of manganese with perovskite structure. *Physica, 16*, 337.

Julliere, M. (1975). Tunneling between ferromagnetic films. *Physics Letters A, 54*, 225.

Kasuya, T. (1956). A theory of metallic ferromagnetism and antiferromagnetism on Zeners model. *Progress of Theoretical Physics, 16*, 45.

Kim, D. H., Lee, H. N., Varela, M., & Christen, H. M. (2006). Antiferroelectricity in multiferroic $BiCrO_3$ epitaxial films. *Applied Physics Letters, 89*, 162904.

Kimura, T., Goto, T., Shintani, H., Ishizaka, K., Arima, T., & Tokura, Y. (2003). Magnetic control of ferroelectric polarization. *Nature, 426*, 55.

Kimura, T., Lawes, G., Goto, T., Tokura, Y., & Ramirez, A. P. (2005). Magnetoelectric phase diagrams of orthorhombic $RMnO_3$ (R = Gd, Tb, and Dy). *Physical Review B, 71*, 224425.

Kiselev, S. V., Ozerov, R. P., & Zhdanov, G. S. (1963). Detection of magnetic order in ferroelectric $BiFeO_3$ by Neutron diffraction. *Soviet Physics Doklady, 7*, 742.

Kleveland, K., Orlovskaya, N., Grande, T., Moe, A. M. M., Einarsrud, M.-A., Breder, K., et al. (2001). Ferroelastic behavior of $LaCoO_3$-based ceramics. *Journal of the American Ceramic Society, 84*, 2029.

Klie, R. F., Yuan, T., Tanase, M., Yang, G., & Ramasse, Q. (2010). Direct measurement of ferromagnetic ordering in biaxially strained $LaCoO_3$ thin films. *Applied Physics Letters, 96*, 082510.

Kobayashi, K. I., Kimura, T., Sawada, H., Terakura, K., & Tokura, Y. (1998). Room-temperature magnetoresistance in an oxide material with an ordered double-perovskite structure. *Nature, 395*, 677.

Kobayashi, K. I., Kimura, T., Tomioka, Y., Sawada, H., Terakura, K., & Tokura, Y. (1999). Intergrain tunneling magnetoresistance in polycrystals of the ordered double perovskite Sr_2FeReO_6. *Physical Review B, 59*, 11159.

Koster, G., Klein, L., Siemons, W., Rijnders, G., Dodge, J. S., Eom, C.-B., et al. (2012). Structure, physical properties, and applications of $SrRuO_3$ thin films. *Reviews of Modern Physics, 84*, 253.

Kramers, H. A. (1934). The interaction between the magnetogenic atoms in a paramagnetic crystal. *Physica, 1*, 182.

Kumar, Y., Choudhary, R. J., & Kumar, R. (2012). Strain controlled systematic variation of metal-insulator transition in epitaxial $NdNiO_3$ thin films. *Journal of Applied Physics, 112*, 073718.

Kumar, A., Martin, L. W., Denev, S., Kortright, J. B., Suzuki, Y., Ramesh, R., et al. (2007). Polar and magnetic properties of $PbVO_3$ thin films. *Physical Review B, 75*, 060101R.

Kumar, A., Pandya, D. K., & Chaudhary, S. (2013). Structural, electronic, and magnetic behavior of two dimensional epitaxial Fe_3O_4/TiN/Si(100) system. *Applied Physics Letters, 102*, 152406.

Kushima, A., Yip, S., & Yildiz, B. (2010). Competing strain effects in reactivity of $LaCoO_3$ with oxygen. *Physical Review B, 82*, 115435.

Kwon, C., Robson, M. C., Kim, K. C., Gu, J. Y., Lofland, S. E., Bhagat, S. M., et al. (1997). Stress-induced effects in epitaxial $(La_{0.7}Sr_{0.3})MnO_3$ films. *Journal of Magnetism and Magnetic Materials, 172*, 229.

Laughlin, D. E., Willard, M. A., & McHenry, M. E. (2000). *Presented at the phase transformations and evolutions in materials*. Warrendale, PA.

Lee, J. S., Arena, D. A., Yu, P., Nelson, C. S., Fan, R., Kinane, C. J., et al. (2010). Hidden magnetic configuration in epitaxial $La_{1-x}Sr_xMnO_3$ films. *Physical Review Letters, 105*, 257204.

Lee, M. J., Park, Y., Suh, D. S., Lee, E. H., Seo, S., Kim, D. C., et al. (2007). Two series oxide resistors applicable to high speed and high density nonvolatile memory. *Advanced Materials, 19*, 3919.

Lee, S., Pirogov, A., Kang, M., Jang, K.-H., Yonemura, M., Kamiyama, T., et al. (2008). Giant magneto-elastic coupling in multiferroic hexagonal manganites. *Nature, 451*, 805.

Lee, D., Yoon, A., Jang, S. Y., Yoon, J. G., Chung, J. S., Kim, M., et al. (2011). Giant flexoelectric effect in ferroelectric epitaxial thin films. *Physical Review Letters, 107*, 057602.

Leusink, D. P., Coneri, F., Hoek, M., Turner, S., Idrissi, H., Van Tendeloo, G., & Hilgenkamp, H. (2014). Thin films of the spin ice compound $HO_2Ti_2O_7$. *APL Materials, 2*, 032101.

Li, P., Guo, B. L., & Bai, H. L. (2011). Spin injection from epitaxial Fe_3O_4 films to ZnO films. *Journal of Applied Physics, 109*, 013908.

Li, X. W., Gupta, A., Xiao, G., Qian, W., & Dravid, V. P. (1998). Fabrication and properties of heteroepitaxial magnetite (Fe_3O_4) tunnel junctions. *Applied Physics Letters, 73*, 3282.

Lisfi, A., Williams, C. M., Nguyen, L. T., Lodder, J. C., Coleman, A., Corcoran, H., et al. (2007). Reorientation of magnetic anisotropy in epitaxial cobalt ferrite thin films. *Physical Review B, 76*, 054405.

Liu, J., Kareev, M., Gray, B., Kim, J. W., Ryan, P., Dabrowski, B., et al. (2010). Strain-mediated metal-insulator transition in epitaxial ultrathin films of $NdNiO_3$. *Applied Physics Letters, 96*, 233110.

Lottermoser, T., Lonkai, T., Amann, U., Hohlwein, D., Ihringer, J., & Fiebig, M. (2004). Magnetic phase control by an electric field. *Nature, 430*, 541.

Lu, Y. X., Claydon, J. S., Ahmad, E., Xu, Y. B., Ali, M., Hickey, B. J., et al. (2005). Hybrid Fe_3O_4/GaAs(100) structure for spintronics. *Journal of Applied Physics, 97*, 10C313.

Lu, Y. X., Claydon, J. S., Xu, Y. B., Thompson, S. M., Wilson, K., & van der Laan, G. (2004). Epitaxial growth and magnetic properties of half-metallic Fe_3O_4 on GaAs(100). *Physical Review B, 70*, 233304.

Luders, U., Bibes, M., Bobo, J. F., Cantoni, M., Bertacco, R., & Fontcuberta, J. (2005). Enhanced magnetic moment and conductive behavior in $NiFe_2O_4$ spinel ultrathin films. *Physical Review B, 71*, 134419.

Luders, U., Bibes, M., Bouzehouane, K., Jacquet, E., Contour, J. P., Fusil, S., et al. (2006). Spin filtering through ferrimagnetic $NiFe_2O_4$ tunnel barriers. *Applied Physics Letters, 88*, 082505.

Luders, U., Sheets, W. C., David, A., Prellier, W., & Fresard, R. (2009). Room-temperature magnetism in $LaVO_3/SrVO_3$ superlattices by geometrically confined doping. *Physical Review B, 80*, 241102.

Lueken, H. (2008). A magnetoelectric effect in $YMnO_3$ and $HoMnO_3$. *Angewandte Chemie International Edition, 47*, 8562.

Lukashev, P., & Sabirianov, R. F. (2010). Flexomagnetic effect in frustrated triangular magnetic structures. *Physical Review B, 82*, 094417.

Lu, Y., Li, X. W., Gong, G. Q., Xiao, G., Gupta, A., Lecoeur, P., et al. (1996). Large magnetotunneling effect at low magnetic fields in micrometer-scale epitaxial $La_{0.67}Sr_{0.33}MnO_3$ tunnel junctions. *Physical Review B, 54*, R8357.

Lu, J., West, K., & Wolf, S. (2010). Novel magnetic oxide thin films. In S. Ramanathan (Ed.), *Thin film metal-oxides* (p. 95). New York: Springer US.

Majkrzak, C. F. (1996). Neutron scattering studies of magnetic thin films and multilayers. *Physica B, 221*, 342.

Maksymovych, P., Huijben, M., Pan, M., Jesse, S., Balke, N., Chu, Y.-H., et al. (2012). Ultrathin limit and dead-layer effects in local polarization switching of $BiFeO_3$. *Physical Review B, 85*, 014119.

Mallinson, J. C. (1993). Magnetic recording media. In J. C. Mallinson (Ed.), *The foundations of magnetic recording* (2nd ed.). (p. 29). Oxford: Academic Press.

Manfred, F. (2005). Revival of the magnetoelectric effect. *Journal of Physics D: Applied Physics, 38*, R123.

Mangalam, R. V. K., Karthik, J., Damodaran, A. R., Agar, J. C., & Martin, L. W. (2013). Unexpected Crystal and domain structures and properties in compositionally graded $PbZr_{1-x}Ti_xO_3$ thin films. *Advanced Materials, 25*, 1761.

Margulies, D. T., Parker, F. T., Rudee, M. L., Spada, F. E., Chapman, J. N., Aitchison, P. R., et al. (1997). Origin of the anomalous magnetic behaviour in single crystal Fe_3O_4 films. *Physical Review Letters, 79*, 5162.

Margulies, D. T., Parker, F. T., Spada, F. E., Goldman, R. S., Li, J., Sinclair, R., et al. (1996). Anomalous moment and anisotropy behavior in Fe_3O_4 films. *Physical Review B, 53*, 9175.

María Luisa, M. (1997). Structural, magnetic and electronic properties of $RNiO_3$ perovskites (R = rare earth). *Journal of Physics: Condensed Matter, 9*, 1679.

Martin, L. W., Chu, Y. H., & Ramesh, R. (2010). Advances in the growth and characterization of magnetic, ferroelectric, and multiferroic oxide thin films. *Materials Science and Engineering: R: Reports, 68*, 89.

Martin, L. W., Crane, S. P., Chu, Y. H., Holcomb, M. B., Gajek, M., Huijben, M., et al. (2008). Multiferroics and magnetoelectrics: thin films and nanostructures. *Journal of Physics: Condensed Matter, 20*, 434220.

Martin, L. W., & Ramesh, R. (2012). Multiferroic and magnetoelectric heterostructures. *Acta Materialia, 60*, 2449.

Martin, L. W., & Schlom, D. G. (2012). Advanced synthesis techniques and routes to new single-phase multiferroics. *Current Opinion in Solid State & Materials Science, 16*, 199.

Martin, L. W., Zhan, Q., Suzuki, Y., Ramesh, R., Chi, M., Browning, N., et al. (2007). Growth and structure of $PbVO_3$ thin films. *Applied Physics Letters, 90*, 062903.

Matzen, S., Moussy, J. B., Mattana, R., Bouzehouane, K., Deranlot, C., & Petroff, F. (2012). Nanomagnetism of cobalt ferrite-based spin filters probed by spin-polarized tunneling. *Applied Physics Letters, 101*, 042409.

Matzen, S., Moussy, J. B., Miao, G. X., & Moodera, J. S. (2013). Direct evidence of spin filtering across $MnFe_2O_4$ tunnel barrier by Meservey-Tedrow experiment. *Physical Review B, 87*, 184422.

Mehta, V. V., Liberati, M., Wong, F. J., Chopdekar, R. V., Arenholz, E., & Suzuki, Y. (2009). Ferromagnetism in tetragonally distorted $LaCoO_3$ thin films. *Journal of Applied Physics, 105*, 07E503.

Meijer, G. I. (2008). Who wins the nonvolatile memory race? *Science, 319*, 1625.

Millis, A. J., Darling, T., & Migliori, A. (1998). Quantifying strain dependence in "colossal" magnetoresistance manganites. *Journal of Applied Physics, 83*, 1588.

Moriya, T. (1960). Anisotropic superexchange interaction and weak ferromagnetism. *Physical Review, 120*, 91.

Moussy, J. B., Gota, S., Bataille, A., Guittet, M. J., Gautier-Soyer, M., Delille, F., et al. (2004). Thickness dependence of anomalous magnetic behavior in epitaxial Fe_3O_4(111) thin films: effect of density of antiphase boundaries. *Physical Review B, 70*, 174448.

Moyer, J. A., Kumah, D. P., Vaz, C. A. F., Arena, D. A., & Henrich, V. E. (2013). Role of epitaxial strain on the magnetic structure of Fe-doped $CoFe_2O_4$. *Journal of Magnetism and Magnetic Materials, 345*, 180.

Moyer, J. A., Vaz, C. A. F., Arena, D. A., Kumah, D., Negusse, E., & Henrich, V. E. (2011). Magnetic structure of Fe-doped $CoFe_2O_4$ probed by x-ray magnetic spectroscopies. *Physical Review B, 84*, 054447.

Moyer, J. A., Vaz, C. A. F., Kumah, D. P., Arena, D. A., & Henrich, V. E. (2012). Enhanced magnetic moment in ultrathin Fe-doped $CoFe_2O_4$ films. *Physical Review B, 86*, 174404.

Moyer, J. A., Vaz, C. A. F., Negusse, E., Arena, D. A., & Henrich, V. E. (2011). Controlling the electronic structure of $Co_{1-x}Fe_{2+x}O_4$ thin films through iron doping. *Physical Review B, 83*, 035121.

Murakami, M., Fujino, S., Lim, S. H., Long, C. J., Salamanca-Riba, L. G., Wuttig, M., et al. (2006). Fabrication of multiferroic epitaxial $BiCrO_3$ thin films. *Applied Physics Letters, 88*, 152902.

Naftalis, N., Kaplan, A., Schultz, M., Vaz, C. A. F., Moyer, J. A., Ahn, C. H., et al. (2011). Field-dependent anisotropic magnetoresistance and planar hall effect in epitaxial magnetite thin films. *Physical Review B, 84*, 094441.

Néel, L. (1932). Influence des fluctuations du champ moléculaire sur les propriétés magnétiques des corps. *Annales de Physique, 18*, 5.

Nogués, J., & Schuller, I. K. (1999). Exchange bias. *Journal of Magnetism and Magnetic Materials, 192*, 203.

Novojilov, M. A., Gorbenko, O. Y., Graboy, I. E., Kaul, A. R., Zandbergen, H. W., Babushkina, N. A., et al. (2000). Perovskite rare-earth nickelates in the thin-film epitaxial state. *Applied Physics Letters, 76*, 2041.

Ogale, S. B., Ghosh, K., Sharma, R. P., Greene, R. L., Ramesh, R., & Venkatesan, T. (1998). Magnetotransport anisotropy effects in epitaxial magnetite (Fe_3O_4) thin films. *Physical Review B, 57*, 7823.

Ohshima, E., Saya, Y., Nantoh, M., & Kawai, M. (2000). Synthesis and magnetic property of the perovskite $Bi_{1-x}Sr_xMnO_3$ thin film. *Solid State Communications, 116*, 73.

Ohtomo, A., & Hwang, H. Y. (2004). A high-mobility electron gas at the $LaAlO_3/SrTiO_3$ heterointerface. *Nature, 427*, 423.

Özgür, Ü., Alivov, Y. I., Liu, C., Teke, A., Reshchikov, M. A., Doğan, S., et al. (2005). A comprehensive review of ZnO materials and devices. *Journal of Applied Physics, 98*, 041301.

Park, J. H., Lee, J. H., Kim, M. G., Jeong, Y. K., Oak, M. A., Jang, H. M., et al. (2010). In-plane strain control of the magnetic remanence and cation-charge redistribution in $CoFe_2O_4$ thin film grown on a piezoelectric substrate. *Physical Review B, 81*, 134401.

Park, J. H., Vescovo, E., Kim, H. J., Kwon, C., Ramesh, R., & Venkatesan, T. (1998). Magnetic properties at surface boundary of a half-metallic ferromagnet $La_{0.7}Sr_{0.3}MnO_3$. *Physical Review Letters, 81*, 1953.

Penicaud, M., Siberchicot, B., Sommers, C. B., & Kubler, J. (1992). Calculated electronic band structure and magnetic moments of ferrites. *Journal of Magnetism and Magnetic Materials, 103*, 212.

Philipp, J. B., Reisinger, D., Schonecke, M., Marx, A., Erb, A., Alff, L., et al. (2001). Spin-dependent transport in the double-perovskite Sr_2CrWO_6. *Applied Physics Letters, 79*, 3654.

Preisler, E. J., Brooke, J., Oldham, N. C., & McGill, T. C. (2003). Pulsed laser deposition growth of Fe_3O_4 on III-V semiconductors for spin injection. *Journal of Vacuum Science and Technology B, 21*, 1745.

Prellier, W., Haghiri-Gosnet, A. M., Mercey, B., Lecoeur, P., Hervieu, M., Simon, C., et al. (2000). Spectacular decrease of the melting magnetic field in the charge-ordered state of $Pr_{0.5}Ca_{0.5}MnO_3$ films under tensile strain. *Applied Physics Letters, 77*, 1023.

Prellier, W., Lecoeur, P., & Mercey, B. (2001). Colossal-magnetoresistive manganite thin films. *Journal of Physics: Condensed Matter, 13*, R915.

Prellier, W., Singh, M. P., & Murugavel, P. (2005). The single-phase multiferroic oxides: from bulk to thin film. *Journal of Physics: Condensed Matter, 17*, R803.

Qiu, Z. Q., & Bader, S. D. (2000). Surface magneto-optic Kerr effect. *Review of Scientific Instruments, 71*, 1243.

Qu, T. L., Zhao, Y. G., Yu, P., Zhao, H. C., Zhang, S., & Yang, L. F. (2012). Exchange bias effects in epitaxial $Fe_3O_4/BiFeO_3$ heterostructures. *Applied Physics Letters, 100*, 242410.

Ramesh, R., & Spaldin, N. A. (2007). Multiferroics: progress and prospects in thin films. *Nature Materials, 6*, 21.

Ramirez, A. P., Hayashi, A., Cava, R. J., Siddharthan, R., & Shastry, B. S. (1999). Zero-point entropy in 'spin ice'. *Nature, 399*, 333.

Ramos, A. V., Guittet, M. J., Moussy, J. B., Mattana, R., Deranlot, C., Petroff, F., et al. (2007). Room temperature spin filtering in epitaxial cobalt-ferrite tunnel barriers. *Applied Physics Letters, 91*, 122107.

Ramos, A. V., Santos, T. S., Miao, G. X., Guittet, M. J., Moussy, J. B., & Moodera, J. S. (2008). Influence of oxidation on the spin-filtering properties of $CoFe_2O_4$ and the resultant spin polarization. *Physical Review B, 78*, 180402R.

Rao, C. N. R., & Raveau, B. (1998). *Colossal magnetoresistance, charge ordering and related properties of manganese oxides*. Singapore: World Scientific.

Rigato, F., Geshev, J., Skumryev, V., & Fontcuberta, J. (2009). The magnetization of epitaxial nanometric $CoFe_2O_4$(001) layers. *Journal of Applied Physics, 106*, 113924.

Rigato, F., Piano, S., Foerster, M., Giubileo, F., Cucolo, A. M., & Fontcuberta, J. (2010). Andreev reflection in ferrimagnetic $CoFe_2O_4$ spin filters. *Physical Review B, 81*, 174415.

Ruderman, M. A., & Kittel, C. (1954). Indirect exchange coupling of nuclear magnetic moments by conduction electrons. *Physical Review, 96*, 99.

Saerbeck, T., & Klose, F. (2012). Neutron scattering and its application to investigate magnetic thin film structures. *Iumrs International Conference in Asia 2011, 36*, 488.

Sai, N., Fennie, C. J., & Demkov, A. A. (2009). Absence of critical thickness in an ultrathin improper ferroelectric film. *Physical Review Letters, 102*, 107601.

Sakai, M., Masuno, A., Kan, D., Hashisaka, M., Takata, K., Azuma, M., et al. (2007). Multiferroic thin film of Bi_2NiMnO_6 with ordered double-perovskite structure. *Applied Physics Letters, 90*, 072903.

Sanchez, F., Bachelet, R., de Coux, P., Warot-Fonrose, B., Skumryev, V., Tarnawska, L., et al. (2011). Domain matching epitaxy of ferrimagnetic $CoFe_2O_4$ thin films on Sc_2O_3/Si(111). *Applied Physics Letters, 99*, 211910.

Sando, D., Agbelele, A., Rahmedov, D., Liu, J., Rovillain, P., Toulouse, C., et al. (2013). Crafting the magnonic and spintronic response of $BiFeO_3$ films by epitaxial strain. *Nature Materials, 12*, 641.

Scherwitzl, R., Zubko, P., Lezama, I. G., Ono, S., Morpurgo, A. F., Catalan, G., et al. (2010). Electric-field control of the metal-insulator transition in ultrathin $NdNiO_3$ films. *Advanced Materials, 22*, 5517.

Schmid, H. (1994). Multi-ferroic magnetoelectrics. *Ferroelectrics, 162*, 317.

Schmidt, G., Ferrand, D., Molenkamp, L. W., Filip, A. T., & van Wees, B. J. (2000). Fundamental obstacle for electrical spin injection from a ferromagnetic metal into a diffusive semiconductor. *Physical Review B, 62*, R4790.

Schreyer, A., Schmitte, T., Siebrecht, R., Bodeker, P., Zabel, H., Lee, S. H., et al. (2000). Neutron scattering on magnetic thin films: pushing the limits (invited). *Journal of Applied Physics, 87*, 5443.

Schrupp, D., Sing, M., Tsunekawa, M., Fujiwara, H., Kasai, S., Sekiyama, A., et al. (2005). High-energy photoemission on Fe_3O_4: small polaron physics and the Verwey transition. *Europhysics Letters, 70*, 789.

Schuster, C., Luders, U., Fresard, R., & Schwingenschlogl, U. (2013). Lattice relaxation and ferromagnetic character of $(LaVO_3)_m/SrVO_3$ superlattices. *Europhysics Letters, 103*, 37003.

Seidel, J., Singh-Bhalla, G., He, Q., Yang, S.-Y., Chu, Y.-H., & Ramesh, R. (2012). Domain wall functionality in $BiFeO_3$. *Phase Transitions, 86*, 53.

Sharma, M., Gazquez, J., Varela, M., Schmitt, J., & Leighton, C. (2011). Coercivity enhancement driven by interfacial magnetic phase separation in $SrTiO_3(001)/Nd_{0.5}Sr_{0.5}CoO_3$. *Physical Review B, 84*, 024417.

Shiozaki, R., Takenaka, K., Sawaki, Y., & Sugai, S. (2001). Effect of oxygen annealing on the electrical properties of $La_{1-x}Sr_xMnO_{3+\delta}$ single crystals around the compositional metal-insulator transition. *Physical Review B, 63*, 184419.

Shukla, D. K., Kumar, R., Sharma, S. K., Thakur, P., Choudhary, R. J., Mollah, S., et al. (2009). Thin film growth of multiferroic $BiMn_2O_5$ using pulsed laser ablation and its characterization. *Journal of Physics D: Applied Physics, 42*, 125304.

Skumryev, V., Laukhin, V., Fina, I., Marti, X., Sanchez, F., Gospodinov, M., et al. (2011). Magnetization reversal by electric-field decoupling of magnetic and ferroelectric domain Walls in multiferroic-based heterostructures. *Physical Review Letters, 106*, 057206.

Slick, P. I. (1980). Ferrites for non-microwave applications. In E. P. Wohlfarth (Ed.), *Ferromagnetic materials: A handbook on the properties of magnetically ordered substances* (p. 189). Amsterdam: North-Holland Publishing Company.

Slonczewski, J. C. (1958a). Origin of magnetic anisotropy in $Co_xFe_{3-x}O_4$. *Journal of Applied Physics, 29*, 448.

Slonczewski, J. C. (1958b). Origin of magnetic anisotropy in cobalt-substituted magnetite. *Physical Review, 110*, 1341.

Smit, J., & Wijn, H. P. J. (1959). *Ferrites: Physical properties of ferrimagnetic oxides in relation to their technical applications*. New York: John Wiley and Sons.

Sofin, R. G. S., Arora, S. K., & Shvets, I. V. (2011). Positive antiphase boundary domain wall magnetoresistance in Fe_3O_4 (110) heteroepitaxial films. *Physical Review B, 83*, 134436.

Sosnowska, I., Peterlinneumaier, T., & Steichele, E. (1982). Spiral magnetic ordering in bismuth ferrite. *Journal of Physics C: Solid State Physics, 15*, 4835.

Sterbinsky, G. E., Ryan, P. J., Kim, J. W., Karapetrova, E., Ma, J. X., Shi, J., et al. (2012). Local atomic and electronic structures of epitaxial strained $LaCoO_3$ thin films. *Physical Review B, 85*, 020403.

Stöhr, J., Padmore, H. A., Anders, S., Stammler, T., & Scheinfein, M. R. (1998). Principles of X-ray magnetic dichroism spectromicroscopy. *Surface Review and Letters, 5*, 1297.

Stöhr, J., & Siegmann, H. C. (2006). *Magnetism: From fundamentals to nanoscale dynamics*. Berlin: Springer.

Sun, J. Z., KrusinElbaum, L., Duncombe, P. R., Gupta, A., & Laibowitz, R. B. (1997). Temperature dependent, non-ohmic magnetoresistance in doped perovskite manganate trilayer junctions. *Applied Physics Letters, 70*, 1769.

Suzuki, Y., Hu, G., van Dover, R. B., & Cava, R. J. (1999). Magnetic anisotropy of epitaxial cobalt ferrite thin films. *Journal of Magnetism and Magnetic Materials, 191*, 1.

Suzuki, Y., vanDover, R. B., Gyorgy, E. M., Phillips, J. M., Korenivski, V., Werder, D. J., et al. (1996). Structure and magnetic properties of epitaxial spinel ferrite thin films. *Applied Physics Letters, 68*, 714.

Szotek, Z., Temmerman, W. M., Kodderitzsch, D., Svane, A., Petit, L., & Winter, H. (2006). Electronic structures of normal and inverse spinel ferrites from first principles. *Physical Review B, 74*, 174431.

Tachiki, M. (1960). Origin of the magnetic anisotropy energy of cobalt ferrite. *Progress of Theoretical Physics, 23*, 1055.

Takagi, H., & Hwang, H. Y. (2010). An emergent change of phase for electronics. *Science, 327*, 1601.

Takahashi, Y. K., Kasai, S., Furubayashi, T., Mitani, S., Inomata, K., & Hono, K. (2010). High spin-filter efficiency in a Co ferrite fabricated by a thermal oxidation. *Applied Physics Letters, 96*, 072512.

Takaobushi, J., Tanaka, H., Kawai, T., Ueda, S., Kim, J.-J., Kobata, M., et al. (2006). $Fe_{3-x}Zn_xO_4$ thin film as tunable high Curie temperature ferromagnetic semiconductor. *Applied Physics Letters, 89*, 242507.

Teague, J. R., Gerson, R., & James, W. J. (1970). Dielectric hysteresis in single crystal $BiFeO_3$. *Solid State Communications, 8*, 1073.

Tebano, A., Orsini, A., Di Castro, D., Medaglia, P. G., & Balestrino, G. (2010). Interplay between crystallographic orientation and electric transport properties in $La_{2/3}Sr_{1/3}MnO_3$ films. *Applied Physics Letters, 96*, 092505.

Terashima, T., & Bando, Y. (1987). Formation and magnetic properties of artificial superlattice of CoO-Fe_3O_4. *Thin Solid Films, 152*, 455.

Tiwari, A., Jin, C., & Narayan, J. (2002). Strain-induced tuning of metal−insulator transition in $NdNiO_3$. *Applied Physics Letters, 80*, 4039.

Tobin, J. G., Morton, S. A., Yu, S. W., Waddill, G. D., Schuller, I. K., & Chambers, S. A. (2007). Spin resolved photoelectron spectroscopy of Fe_3O_4: the case against half-metallicity. *Journal of Physics: Condensed Matter, 19*, 315218.

Tokura, Y. (2000). *Colossal magnetoresistive oxides*. Amsterdam: Gordon and Breach Science.

Tokura, Y., & Nagaosa, N. (2000). Orbital physics in transition-metal oxides. *Science, 288*, 462.

Torrance, J. B., Lacorre, P., Nazzal, A. I., Ansaldo, E. J., & Niedermayer, C. (1992). Systematic study of insulator-metal transitions in perovskites $R$$NiO_3$ (R=Pr,Nd,Sm,Eu) due to closing of charge-transfer gap. *Physical Review B, 45*, 8209.

Tripathy, D., Adeyeye, A. O., Boothroyd, C. B., & Piramanayagam, S. N. (2007). Magnetic and transport properties of Co-doped Fe_3O_4 films. *Journal of Applied Physics, 101*, 013904.

Urushibara, A., Moritomo, Y., Arima, T., Asamitsu, A., Kido, G., & Tokura, Y. (1995). Insulator-metal transition and giant magnetoresistance in $La_{1-x}Sr_xMnO_3$. *Physical Review B, 51*, 14103.

Van Aken, B. B., Palstra, T. T. M., Filippetti, A., & Spaldin, N. A. (2004). The origin of ferroelectricity in magnetoelectric $YMnO_3$. *Nature Materials, 3*, 164.

van der Zaag, P. J., Ball, A. R., Feiner, L. F., Wolf, R. M., & van der Heijden, P. A. A. (1996). Exchange biasing in MBE grown Fe_3O_4/CoO bilayers: the antiferromagnetic layer thickness dependence. *Journal of Applied Physics, 79*, 5103.

Venkateshvaran, D., Althammer, M., Nielsen, A., Geprags, S., Rao, M. S. R., et al. (2009). Epitaxial $Zn_xFe_{3-x}O_4$ thin films: a spintronic material with tunable electrical and magnetic properties. *Physical Review B, 79*, 134405.

Verschuur, G. L. (1993). *Hidden attraction: The mystery and history of magnetism*. Oxford: Oxford University Press.

Verwey, E. J. W. (1939). Electronic conduction of magnetite (Fe_3O_4) and its transition point at low temperatures. *Nature, 144*, 327.

Viret, M., Drouet, M., Nassar, J., Contour, J. P., Fermon, C., & Fert, A. (1997). Low-field colossal magnetoresistance in manganite tunnel spin valves. *Europhysics Letters, 39*, 545.

Voogt, F. C., Palstra, T. T. M., Niesen, L., Rogojanu, O. C., James, M. A., & Hibma, T. (1998). Superparamagnetic behavior of structural domains in epitaxial ultrathin magnetite films. *Physical Review B, 57*, R8107.

Vullum, P. E., Holmestad, R., Lein, H. L., Mastin, J., Einarsrud, M. A., & Grande, T. (2007). Monoclinic ferroelastic domains in $LaCoO_3$-based perovskites. *Advanced Materials, 19*, 4399.

Vullum, P. E., Lein, H. L., Einarsrud, M. A., Grande, T., & Holmestad, R. (2008). TEM observations of rhombohedral and monoclinic domains in $LaCoO_3$-based ceramics. *Philosophical Magazine, 88*, 1187.

Wolf, S. A., Awschalom, D. D., Buhrman, R. A., Daughton, J. M., von Molnár, S., Roukes, M. L., et al. (2001). Spintronics: a spin-based electronics vision for the future. *Science, 294*, 1488.

Xie, S., Cheng, J., Wessels, B. W., & Dravid, V. P. (2008). Interfacial structure and chemistry of epitaxial $CoFe_2O_4$ thin films on $SrTiO_3$ and MgO substrates. *Applied Physics Letters, 93*, 181901.

Yakel, H. L., Forrat, E. F., Bertaut, E. F., & Koehler, W. C. (1963). On crystal structure of manganese (111) trioxides of heavy lanthanides and yttrium. *Acta Crystallographica, 16*, 957.

Yamamoto, Y., Tanaka, H., & Kawai, T. (2001). The control of cluster-glass transition temperature in spinel-type $ZnFe_2O_{4-\mathrm{delta}}$ thin film. *Japanese Journal of Applied Physics Part 2-Letters, 40*, L545.

Yang, C. H., Koo, T. Y., Lee, S. H., Song, C., Lee, K. B., & Jeong, Y. H. (2006). Orbital ordering and enhanced magnetic frustration of strained $BiMnO_3$ thin films. *Europhysics Letters, 74*, 348.

Yang, Z., Ko, C., & Ramanathan, S. (2011). Oxide electronics utilizing ultrafast metal-insulator transitions. *Annual Review of Materials Research, 41*, 337.

Yang, C.-H., Lee, S.-H., Koo, T. Y., & Jeong, Y. H. (2007). Dynamically enhanced magnetodielectric effect and magnetic-field-controlled electric relaxations in La-doped $BiMnO_3$. *Physical Review B, 75*, 140104R.

Yosida, K. (1957). Magnetic properties of Cu−Mn alloys. *Physical Review, 106*, 893.

Yu, P., Chu, Y. H., & Ramesh, R. (2012). Emergent phenomena at multiferroic heterointerfaces. *Philosophical Transactions of the Royal Society A: Mathematical, Physical and Engineering Sciences, 370*, 4856.

Yu, P., Lee, J. S., Okamoto, S., Rossell, M. D., Huijben, M., Yang, C. H., et al. (2010). Interface ferromagnetism and orbital reconstruction in $BiFeO_3$-$La_{0.7}Sr_{0.3}MnO_3$ heterostructures. *Physical Review Letters, 105*, 027201.

Zavaliche, F., Zheng, H., Mohaddes-Ardabili, L., Yang, S. Y., Zhan, Q., Shafer, P., et al. (2005). Electric field-induced magnetization switching in epitaxial columnar nanostructures. *Nano Letters, 5*, 1793.

Zener, C. (1951). Interaction between the d-shells in the transition metals. II. Ferromagnetic compounds of manganese with perovskite structure. *Physical Review, 82*, 403.

Zhang, Y., Deng, C. Y., Ma, J., Lin, Y. H., & Nan, C. W. (2008). Enhancement in magnetoelectric response in $CoFe_2O_4$-$BaTiO_3$ heterostructure. *Applied Physics Letters, 92*, 062911.

Zhang, Z., & Satpathy, S. (1991). Electron states, magnetism, and the Verwey transition in magnetite. *Physicals Review B, 44*, 13319.

Zhang, W., Zhang, J. Z., Wong, P. K. J., Huang, Z. C., Sun, L., Liao, J. L., et al. (2011). In-plane uniaxial magnetic anisotropy in epitaxial Fe_3O_4-based hybrid structures on GaAs(100). *Physical Review B, 84*, 104451.

Zheng, H., Wang, J., Lofland, S. E., Ma, Z., Mohaddes-Ardabili, L., Zhao, T., et al. (2004). Multiferroic $BaTiO_3$-$CoFe_2O_4$ nanostructures. *Science, 303*, 661.

Zheng, H., Zhan, Q., Zavaliche, F., Sherburne, M., Straub, F., Cruz, M. P., et al. (2006). Controlling self-assembled Perovskite−Spinel nanostructures. *Nano Letters, 6*, 1401.

Ziese, M. (2000). Spontaneous resistivity anisotropy and band structure of $La_{0.7}Ca_{0.3}MnO_3$ and Fe_3O_4 films. *Physical Review B, 62*, 1044.

Ziese, M., & Blythe, H. J. (2000). Magnetoresistance of magnetite. *Journal of Physics: Condensed Matter, 12*, 13.

Zou, X., Wu, J., Wong, P. K. J., Xu, Y. B., Zhang, R., Zhai, Y., et al. (2011). Damping in magnetization dynamics of single-crystal Fe_3O_4/GaN thin films. *Journal of Applied Physics, 109*, 07D341.

Zubko, P., Gariglio, S., Gabay, M., Ghosez, P., & Triscone, J.-M. (2011). Interface physics in complex oxide heterostructures. *Annual Review of Condensed Matter Physics, 2*, 141.